DESIGN OF LIGHT WEIGHT POLYMER BIN FOR HOPPER TIPPER APPLICATION

A thesis submitted in partial fulfilment of the requirement for the award of the degree of

Master of Engineering
in
Thermal Engineering

Submitted by

Manish Singhal
Registration No. 801783009

Under the Supervision of

Dr. Amandeep Singh Oberoi
(Assistant Professor, Mechanical Engineering Department)

Mr. Rajeev Dave
(General Manager, Application Engineering, ERC, TATA Motors Ltd., Pune)
&
Mr. Aneeth P.M
(Senior Manager, Application Engineering, ERC, TATA Motors Ltd., Pune)

THAPAR INSTITUTE
OF ENGINEERING & TECHNOLOGY
(Deemed to be University)

Department of Mechanical Engineering
Thapar Institute of Engineering & Technology, Patiala, Punjab
(Deemed to be University)
July, 2019

CERTIFICATION

This is to certify that the work done in this thesis title **"Design of Light Weight Polymer Bin for Hopper Tipper Application"** submitted in partial fulfilment of requirement for the award of Master of Engineering Degree in Thermal Engineering in the Mechanical Engineering Department of Thapar Institute of Engineering & Technology, is an authentic record of work carried out by me under the guidance of **Dr. Amandeep Singh Oberoi,** Assistant Professor, Mechanical Engineering Department, Thapar Institute of Engineering & Technology, Patiala, **Mr. Rajeev Dave,** General Manager, Application Engineering, ERC, TATA Motors Ltd., Pune and **Mr. Aneeth P.M.** Senior Manager, Application Engineering, ERC, TATA Motors Ltd., Pune. The matter embodied in this report has not been submitted in any part or full to any university or institute for the award of any degree.

26/6/2019

Date: 26/6/19

Manish Singhal
Roll No. 801783009

This is to certify that above declaration made by the student concerned is correct to the best of my knowledge & belief.

28.06.09

Date: 28/6/19

Mr. Rajeev Dave
General Manager, Application Engineering,
ERC, TATA Motors Ltd.,
Pune, Maharashtra.

Date: 26.06.2019

Mr. Aneeth P.M
Senior Manager, Application Engineering,
ERC, TATA Motors Ltd.,
Pune, Maharashtra.

Date: 15.07.2019

Dr. Amandeep Singh Oberoi
Assistant Professor, MED,
T.I.E.T., Patiala, Punjab.

ACKNOWLEDGMENT

I would like to specially acknowledge and extent my heartfelt gratitude to all those who have helped me in completion of this thesis. I especially would like to thank **Mr. Rajeev Dave,** General Manager, Application Engineering, TATA Motors Ltd., **Mr. Aneeth P.M,** Senior Manager, Application Engineering, TATA Motors Ltd., **Dr. Amandeep Singh Oberoi,** Assistant Professor, MED, T.I.E.T. for their full support and guidance.

I would also like to thank my parents for their years of love, support and encouragement in every step of my life. They have always wanted the best for me and I admire their determination and sacrifice. Besides, I would like to acknowledge my institute i.e**. Thapar Institute of Engineering & Technology.** TATA Motors is gratefully acknowledged for providing the best platform for research. My special thanks are due to my TATA family and friends who constantly encourage me to complete this research work.

Last but not the least, I pay my sincere gratitude to Head of Department MED and Dean of Academic affairs for motivating me to complete the work in stipulated time frame.

DATE: 15/07/2019

(Manish Singhal)
M.E. (Thermal)
(801783009)

Table of Contents

LIST OF TABLES

LIST OF FIGURES

LIST OF ABBREVIATIONS

DCPD: Dicyclopentadiene

AHSS: Advanced High Strength Steel

SCV: Small Commercial Vehicle

RIM: Reaction Injection Moulding

TIM: Thermoplastic Injection Moulding

SDOF: Single Degree of Freedom

UDL: Uniform Distributed Load

CAE: Computer Aided Engineering

CES: Cambridge Engineering Selector

UDL: Uniform Distributed Load

FEA: Finite Element Analysis

ABSTRACT

The automobile industry is facing challenges to develop fuel efficient, strict emission norms compiling and durable vehicles. The best solution to meet these challenges is to replace conventional steel by lightweight material in manufacturing various components of a vehicle. There are number of lightweight material available (AHSS, composites, polymers) but polymers are the best choice because of their good mechanical and physical properties. Application of polymer offers design freedom, which is significantly important for the aesthetics of the vehicle. The presented work focuses on investigation of the use of such polymers in manufacturing a hopper for commercial tipper trucks. Investing and testing of a possible solution to the problem stated above is the main objective of this work. This is accomplished by demonstrating, what can be achieved with a polymer-metal stuffed structure of Dicyclopentadiene (DCPD). For this, the hopper tipper of TATA vehicle was used as an object of study. Design, prototyping, mechanical simulation and validation, and environmental impact are herein documented.

The design phase counts on the creation of a hopper tipper models through computer-aided design and engineering software that enabled achieving the optimum required targets in terms of strength, stiffness and weight. Its structural validation was done by a finite element method at the end of each model. The use of DCPD hopper allows reducing weight and tooling. DCPD hopper with stiffener and metal support structure model shows an adequate strength for tipping application. The modal analysis shows a higher frequency for the conversion of mode shape for final designed hopper. The hopper was then fabricated using reaction injection moulding and then fixing on a metallic frame. Hopper and metal supporting structure assembly are completed using fasteners and adhesive bonding.

Keywords: DCPD, Finite element method, Modal analysis, Reaction injection moulding.

Chapter 1: INTRODUCTION AND OBJECTIVES

1.1 Introduction

The automobile industry is currently facing number of challenge to develop future vehicles for market. More market demand of fuel efficient vehicles in same price for all segments passenger and commercial vehicle. In order to meet emission norms there is an inertia class for all vehicles defined as per their engine configuration. New emission norms would be applicable in India. Only selling of low emissions complying vehicle is allowing in Indian market to minimize air pollution in the country. Upcoming strict emission norms are forcing automotive company to develop and use lighter weight material in fabrication of vehicle. Industry is looking for light weight material to improving vehicle efficiency, and thus fuel economy. Theoretically reducing weight of a vehicle by 1/10th could help achieving a six percent enhancement in fuel economy [1]. To meet the consumer's requirements of more fuel economy, the design engineer has to participate and highlight the benefits of all existing engineering options. Some of the engineering options to increasing fuel economy of vehicles are as follows:

I. Increasing powertrain efficiency.
II. Decreased rolling resistance of tires.
III. Improved surface smoothness to reducing air resistant.
IV. Reduced vehicle components Weight.
V. Increased Vehicle electrification efficiency.

Generally, industry preferred weight reduction option with other fuel-economy increasing actions in competitive market.

Manufacturing of engine blocks from cast-aluminum alloy material to meet weight and cost saving targets is used from decades and have now become a part of systematic production in the industry. Similarly, advanced high strength steel (AHSS) sheets are used in manufacturing of vehicle body structure that provides cost saving and weight reduction without compromising on strength. Aluminum has emerged as an attractive material to replace steel finishes (trunk lids, hoods, wind deflector etc.) that offers weight saving and great surface finish. Recently Ford F-150 pickup truck's body got manufactured from aluminum and has shown great market exploitation of advanced materials for vehicle weight saving.

A complete system-engineering approach is used to implement advanced materials in a cost effective way. Just reducing a component weight is not sufficient solution for weight saving and material optimization. We need to change other conventional process is also like manufacturing process, designs etc. Manufacturing processes are different for advanced materials which we review and develop advance manufacturing process to achieve the weight reductions at less price increment to sustain the affordable solution for the automobile.

Figure 1.1 shows weight reduction and cost increment by changing conventional steel with new materials. A Polymer in this series shows a great cost saving than other material options and weight saving of more than advanced high strength steel. Weight reduction by polymer achieved only 4% less than aluminum metal but more cost saving. Generally, Fe410 steel grade is the most common material used in the automobile industry for manufacturing exterior parts because it can offer good stiffness and strength even with less thickness. In recent years' new polymer developed are an attractive choice to weight reduction with multiple benefits.

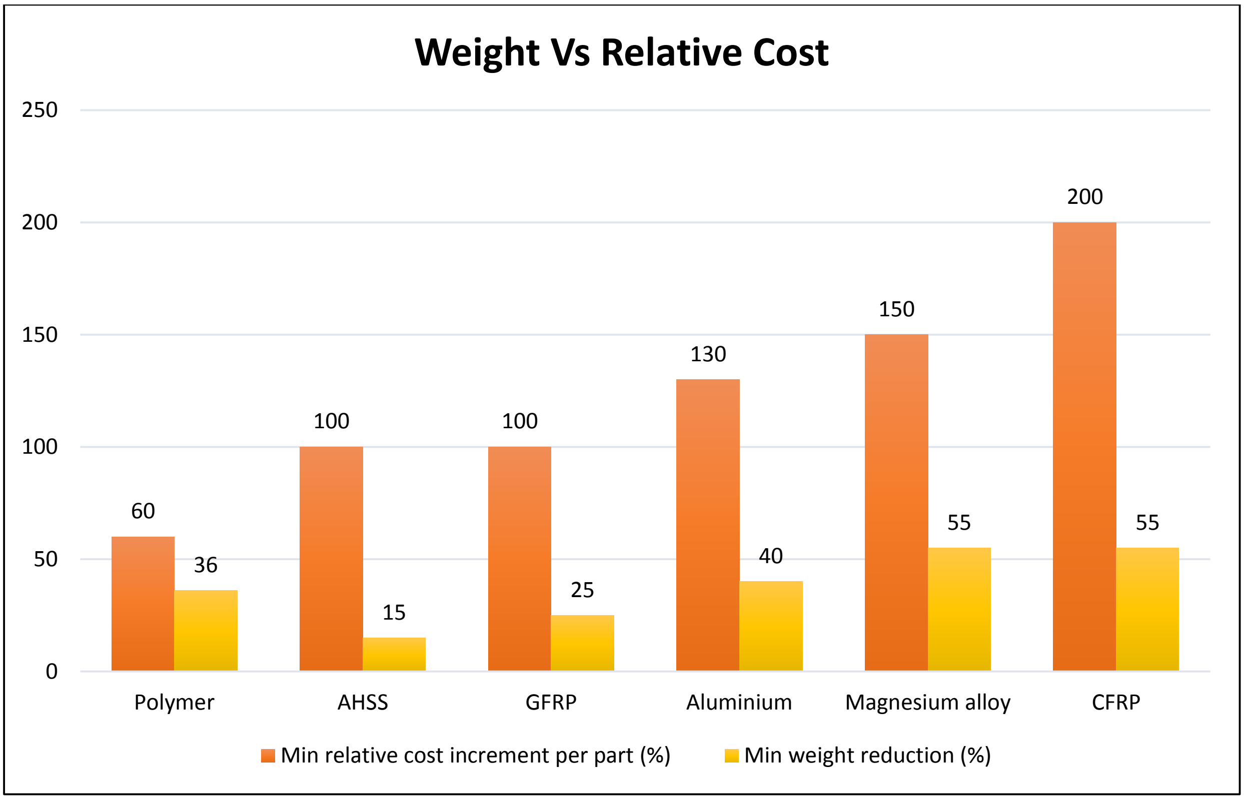

Figure 1.1: Weight Vs Cost of production [1].

Glass fiber and carbon fiber reinforced composites can also be employed as alternative material even involving some engineering challenges. Reinforced composites have attractive property like high strength, corrosion resistance and light weight for a wide range of production volumes (high, medium and low) depending upon composite material production process.

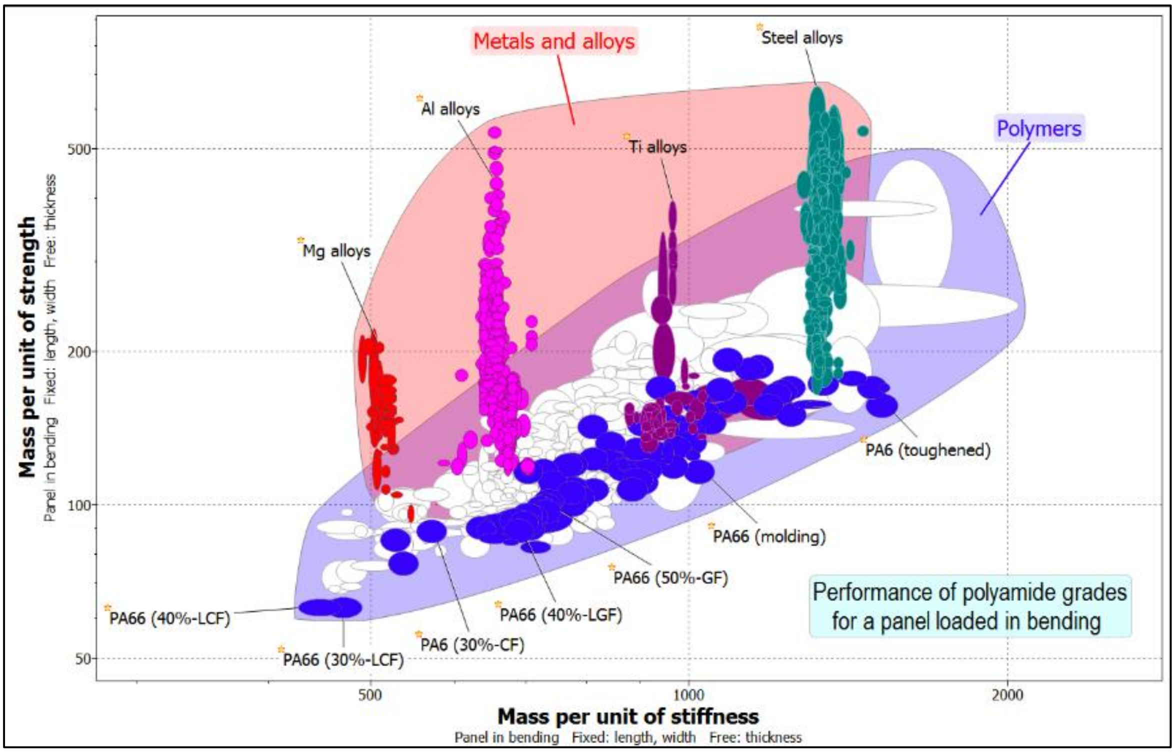

Figure 1.2*: Materials selection using a property chart in CES Selector [2].* *(Ashby, 2007)*

"CES" Selector is developed in Ansys Granta which is very effective tool for systematic rational material selection technique developed by Professor Mike Ashby and Collaborators at university of Cambridge. A fast and easiest way to find material with parallel property profile in reference material and help in making substitutions of materials.

1.2 Family tree of materials

It is established to categorise the materials of engineering into the six wide families shown in Figure 1.2: metals, polymers, elastomers, ceramics, glasses and Hybrids. Hybrids or composite are special material developed by combining two or more other family materials.

Polymers are organic solids because of presence the long carbon chains structure (silicon) atoms. Polymers are in lightweight due to their lesser densities compare to lightest metals. Polymer have low-density because of their most of part made of light atomic weight carbon (Atomic weight: 12) and hydrogen (Atomic weight: 1) in semi-crystalline packings or low-density amorphous. They have roughly 50 times less moduli E than metals. But a polymer is strong enough, because of their low density, their strength to weight ratio is higher than metals. Properties of polymer depend upon the temperature of the environment. Low toughness and flexible property at low temperature (-4°C) polymer become brittle. At high temperature (100°C) polymer become softer or rubbery show less strength and ductile behaviour.

Selection Properties

1. Physical property.
2. Mechanical property.
3. Durability.
4. Price & Availability.
5. Chemical resistant, Abrasion wear.
6. Ease of manufacturing and assembly.
7. Aesthetic, Texture, design, etc.

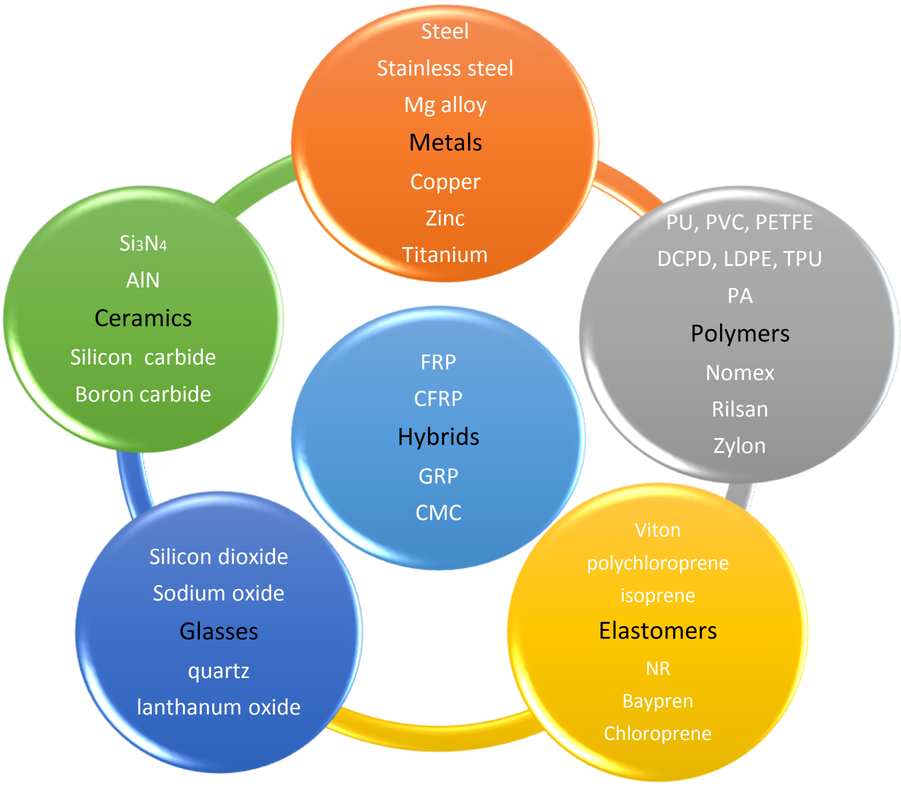

Figure 1.3: Family Tree of Materials.

Polymer materials are an attractive choice to automobile manufacturer for lightweight vehicle components. To reduce vehicle weight polymers also a number of benefits (corrosion resistance, Chemical resistance etc.). A lot of research work on searching the right Polymer for automobile applications. By implementing lightweight polymer that can be easily shaped (to give design freedom for complex shape) technologies with acceptable to the market, production intonations and cost.

High production volume in automobile manufactured used high-cost initial tooling investment, in the current competitive market we need to develop a process to achieve low initial cost tooling manufacturing. For manufacturing car or truck exterior body panels making by metal require high initial cost tooling. Metals exterior panels shall be replaced, reduced and combination of other material, once they reduce preliminary investment in developing tooling process, Initial investment for production contributes 40% of total vehicle cost.

1.3 Motivation

Study of materials (metals and polymers) property for selection of a suitable option to reduce the weight of vehicle component. First study of existing steel use in automobile manufacturing. Fe410 is most common steel used in the manufacturing industry because of low price and easily available.

Table 1. 1: Metals property comparison.

Metals	Density (g/cm^3)	Yield Strength (MPa)	Elongation (%)	Impact Strength Charpy V-Notch (J)
Fe410	7.85	250	17	27
E34		340	27	40
HSLA420		420	23	50
BSK46		460	21	45

Table 1.2: Polymers property comparison.

Polymers	Density (g/cm^3)	Tensile Strength (MPa)	Elongation (%)	Impact Strength	Flexural Modulus (MPa)
DCPD	1.03	43	5	118 (J/m^2)	1850
PA66	1.05	79	10	4.9 (kJ/m^2)	2800
PP	0.89	29	10	18 (J/m^2)	1240
PTFE	2.16	27	300	188 (J/m^2)	340

Polymers material are implemented in vehicle parts (Bumper, exterior body panels, Footsteps, SUPD etc.) to deliver excellent results compare to metals. Lightweight one of the results offers independently on their type (Thermoplastic or Thermoset). By using polymers not only, we get energy saving in the production of vehicle components but also vehicle life itself. Thermoset polymers are cross-linked making them stronger and stiffer than thermoplastic. The Cross – link structures are not broken by heating and make it stronger in harsh condition. Thermoset polymers do not require high injection pressure in the moulding process. Among the range of available thermoset polymer Dicyclopentadiene (DCPD) is superficially choice because of their wonderful mechanical property especially a high toughness which is up to metals.

Molecular dynamics simulation suggest the origin is the lack of strong non-covalent interaction and the facile formation of nanoscale voids to accommodate strain in DCPD.DCPD is widely used in peripheral parts of vehicle body panels for trucks & rough environment working condition of heavy machines in mines and agriculture. Application of DCPD in automobile industry still little investigated, it is a cost-effective solution for replacing metals parts with DCPD compare to Polymers.

Innovation and excellence for mobility Industries are used DCPD material for a Bin. This Bin used for Hopper Tipper application on a small commercial vehicle (SCV) because SCV segment has less payload, dimensions and design complexity. The vehicle is used for municipal waste collection in the city. Door to Door garbage collection have more stoppage, household garbage contains dangerous chemicals, sharp edge metal debris, wet waste. DCPD perfect for all these challenges because of high chemical resistance for great range, toughness, ballistic property, abrasion resistant.

It summarizes also some material, adhesive and assembly technologies expanded in exterior used of Hopper, as well as the state-run of the ability of the DCPD. The part covers all hopper tipper development, including an introduction to the materials used and a detailed report of the design, mechanical simulations, prototyping and testing. Tooling development and ribs design are also covered within this thesis.

Chapter 2: BACKGROUND & LITERATURE REVIEW

2.1 Rationale for the design

Lightweight polymer is playing an important role in the present and future of the automobile industry. The implementation of emission norms and demand for fuel-efficient vehicle emphasises on production of vehicle from lightweight material.

I am highly motivated towards working on the design of polymer or composite materials advancement in recent years due to the many benefits that it offers like durability, lightweight, design freedom and easy assembly. Although some challenges invite the researchers to work on them.

2.2 Literature Review

Placzek M, et al. 2017, studied damping vibration of Power steering made up of DCPD and aluminum alloy. A study was done by comparing damping vibrations of two different types of materials in automobile electrically operated Power steering housing. Existing Power steering housing used in an automobile is composed of Aluminum alloy. Aluminum alloy power steering is manufactured by the conventional method of the metal casting process. Another one is composed of DCPD (Dicyclopentadiene Polymer) which is a new one material in steering housing manufacturing we produced by using the RIM (Reaction Injection moulding) technology. These two steering housing physical model is manufactured for analysis of vibration damping property. Vibration signifies the noise generation in component means more vibration more noise which is indispensable property in automobiles components. Test for measuring vibrations generated by power steering is done by using Macro Fiber Composite piezoelectric transducers. The transducer plate is attached to the surface of the steering housing. Same parameters of excitation vibrations introduced in both DCPD and aluminum alloy power steering.
Comparison of the result shows that DCPD material has less vibration than aluminum alloy. By analyzing the waveforms Damping coefficient of DCPD is higher than aluminum alloy found when the experiment result compared [3].

Margarita K. Zamanova, et al. 2016, the study of friction and wear behaviour of DCPD.The investigation of wear & Frictional behaviour of Polymer (DCPD) contact with steel. Study of wearing of material done with respect to load and roughness. Setup for making a test is pin-on-disc arrangement under dry and boundary lubrication state. These Tribological tests were conducted in these conditions Pressure (10N and 18N).

- Roughness of steel (0.08 μm and 0.15 μm).
- Speed of Disc 0.5 m/s.
- Slipping distance 1300 m.
- At Room temperature (23 ^{o}C).

Results are shown that wear increases with increasing pressure under dry friction sliding condition. More about that setting up of the unevenness of steel from 0.08 µm to 0.15 µm of material twice the wear intensity. By using boundary lubrication friction between DCPD and steel decreased linearly with reduced in viscosity of lubricants (polydimethylsiloxane fluids). DCPD against steel show appropriate wear and friction properties under dry friction and boundary lubrication surface contact.

When an increase in steel disc roughness or applied load coefficient friction coefficient between Steel and DCPD rises insignificantly. By decreasing viscosity of lubricant PML friction also reduced linearly in the presence of boundary lubrication and friction coefficient. Dry friction case shows a more significant effect on friction and wears behaviour of DCPD in a specific range of load and roughness [4].

James Gilford III, et al. 2014, Use of DCPD for self-healing material for concrete blocks. Microcrack in a block of concrete is generated due to high load impact and vibration. To heal these cracks, we fill DCPD and sodium silicate material and analysed the mechanical property of concrete. Analysis of temperature, agitation rate and pH of microcapsules and self-healing mechanism in concrete by doing experiments in the laboratory.
Microcapsule Parametric Analysis Results, the yield for DCPD was found highest 79.0 % at agitation rate 350 rpm, pH 3.7 and a temperature of 55 °C measured. Yield for SS was found 94.9 % at same agitation rate and temperature, pH of 3.2.
The shell thickness of DCPD is almost half of the shell thickness of Sodium silicate. SS microcapsules increases as increase pH. DCPD microcapsules increase as decrease in pH. For DCPD by 30% increment in modulus for microcapsules, healing as prepared pH of 3.1. For Sodium silicate by 11% increment in modulus for microcapsules, healing as prepared pH of 3.1 [5].
Bingli Pana b, et al. 2012, A Test is conducted by using high-speed pin-on-disc tribometer to analyse Dry friction behaviours of the DCPD material in contact with steel at different sliding velocity (5m/s, 10m/s, 15m/s, and 20m/s). Scanning electron microscopy (SEM) instrument

used to observe microstructure changes on the sliding surface of DCPD. The value of friction coefficients increase with increasing sliding velocity means more wear of DCPD surface at the high-speed run of steel. It's observed that coefficients of friction DCPD as sliding velocity of 5m/s were the most constant, and the coefficients of friction were asymmetrical with the further increasing the sliding velocity. SEM results show that abrasive wear of DCPD surface of the sliding velocity of 5m/s and critical adhesive wear at 20m/s sliding speed. At high sliding velocity surface, Heating and temperature rise caused to change the microstructure of the material. The temperature rises of Polymer reason for complicated variation in wearing the degradation of tri-biological properties of couples [6].

The massive wear loss of DCPD increased by 75%, when sliding velocity was changed after 5m/s to 10m/s. When additional changing in sliding velocity increase wear mass loss by 71%. Wear of mass continuously increased with increase in speed of sliding but suddenly increased estimated when velocity increase up 20m/s. It is concluded that DCPD material performs better surface wear property at less than 4m/s.

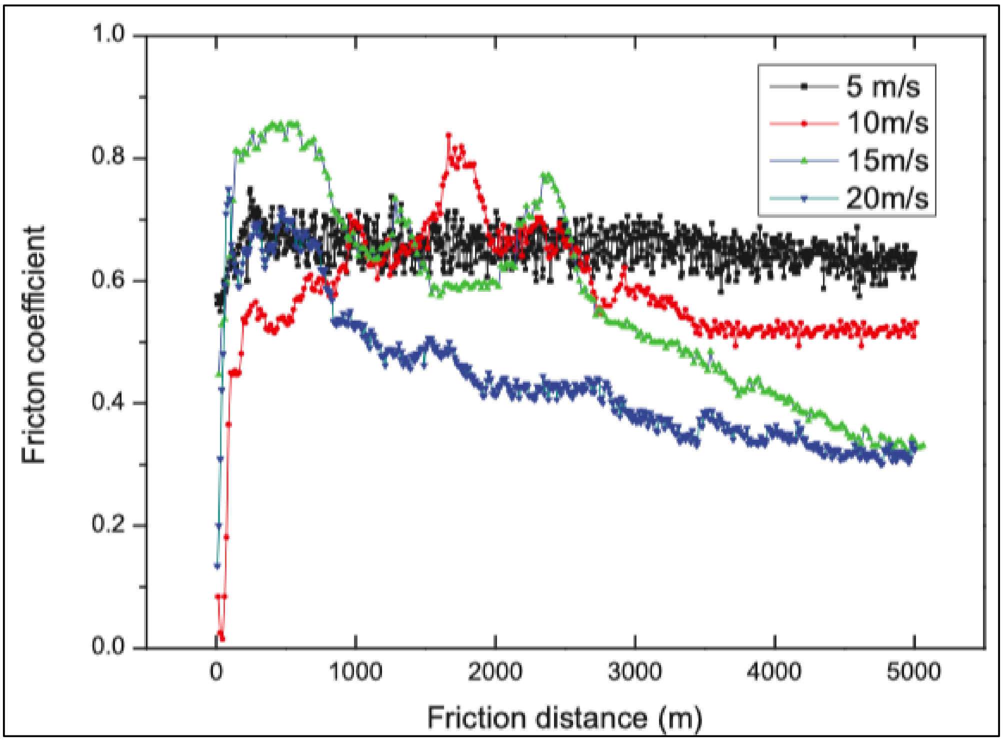

Figure 2.1: Changes in Friction coefficient of DCPD at dry sliding velocity *(Pan, 2012)***.**

Daniel B. Knorr Jr. et al. 2015, Ballistic property comparison of DCPD material with structural epoxy resin. The test is conducted at a high rate of response to projectile penetration Kinetic energy. The kinetic energy describes like 50% of velocity probability of partial penetration.

DCPD test results show excellent penetration resistance with 300 to 400% enhancement in ballistic energy dissipation compared to structural epoxy resins. The reason for showing this much of ballistic performance is cross-linked branched structure of DCPD material at low temperature. This is expected to be a very broad range (-55 to 75C) which suitable for all earth locations. Glass storage modulus of 1.7 GPa offered high energy dissipation trade-off than traditional cross-linked polymer. By using Quasi-static approach DCPD have higher fracture toughness & Lower yield stress compare to typical epoxies & strong non-covalent interaction structure facile formation void to accommodate strain in DCPD. In this test Ballistic impact was carried out with a 0.22 calibre gas gun at different temperature. DCPD polymer show high fracture toughness, low yield strength in tension, and low yield strength in compression.

Mechanical property enhancement by reinforcing metal wire in DCPD [7].

Andre Camboa, et al. 2013, DCPD polymer reinforced by metal wire is an easy way to enhance the strength of the material. Process of manufacturing of wire reinforcement in DCPD in over moulding techniques. Metal insert in polymer has no restriction of the use of different wire materials. Flexural study of material shows very good results of tensile strength and modulus of elasticity. The flexural strength & modulus of elasticity increased by more than three and 5.6 times respectively by inserting metal wire inside the polymer. Weight of metal wire insert is double the weight of DCPD. The density of material increased by double but strength enhancement is more [8].

Shi Xiaorong. 2018, In this patent DCPD material, use to cover structure for the vehicle. Structure equipped with ribs and strips to provide strength and stiffness. The cover used at the external body of the car to protect them from a collision. Damping coefficient of DCPD is high to add safety feature in the car during a collision on road. Ribs are introduced will increase the strength without an increment in weight of the vehicle [9].

Joung-Man Park, et al. 2015, Three types of catalyst were used in DCPD RIM manufacturing. Catalysts W (tungsten), Mo (molybdenum) and Ru (ruthenium) it effects the mechanical and thermal properties. The DCPD material exhibit the heat of reaction at same temperature and no change in heat of reaction with different catalyst but takes curing time differ. The most active catalyst in RIM process of DCPD was tungsten, whereas the slowest was molybdenum due to different catalyst reactions. The mechanical property of DCPD significantly varies as the change in air exposer [10].

2.3 Background

DCPD was firstly used on the manufacturing of exterior components for trucks and agricultural vehicles. It has also been used in the fabrication of snowmobiles, boat housing, chlorine cell covers, wastewater treatment equipment and even cryogenic tanks. Currently, one of the most relevant applications for DCPD is the bin on the new W900L model of Kenworth Truck Co, as can be seen in Figure 2.9. Here DCPD replaced a spray-up GFRC at no additional cost and 38kg weight saving [11].

Figure 2.2: Kenworth Truck bonnet.

Leading companies of world like Mercedes, Caterpillar use DCPD material for manufacturing of external parts of the vehicle like fender, bonnet, wind deflector etc.

Figure 2.3: Vehicle parts made of DCPD material *(Metton, 2010)***.**

TATA Motors designs a sports car with DCPD material the material supply by metton USA. This is the first sports car in the automobile industry whose whole body manufactured by plastic. The Weight advantage of using plastic but also cost savings in material and producing parts. This is the cheapest sports car in the world with full feature loaded.

Racemo is fully developed by lightweight polymer material to accelerate the vehicle quickly. This car takes 4 to 7 secs to reach a speed of 100 Kmph.

Limited production of this car for Tata turnaround 2.0 design concept for innovation. TAMO body structure is the sandwich type to enhance strength and toughness of sports car body.

2.4 Objectives

The purpose of this thesis project is to design a lightweight hopper tipper by using polymer material. The design will be fulfilling the market conditions, load bearing without any failure in a bin. Durability concern in hopper working in rough uses pattern without any degradation of material and failure in operation. Design of bin will be a good aesthetic and easy assembly. Manufacturing concern needs to be taken consideration to make the project feasible in proto planning.

- To reduce the weight of hopper tipper: - The design and development of Hopper Tipper with a lightweight Polymer material. Hopper is assembling in such a way that its weight should be lowest.
- To maintain adequate strength against failure in loaded conditions.:- The mechanical properties of the components should be kept according to the structural quality requirements imposed by ARAI.
- To minimise the number of operations in assembly:- By reducing the number of assembly operations it is expected to decrease both production costs and cycle times.
- To minimize the cost of production:- Cost is one of the most important issues to be analysed herein, once low production volumes are inherent to this kind of vehicles. Thus, the costs of the explored technologies shall remain cost efficient at 3000 units per year.
- To enhance the aesthetics of hopper tipper:- Polymer hopper tipper is manufactured by Reaction injection moulding technique which give design freedom. It is possible to design hopper tipper with varying thickness profile, sudden bending, inbuilt ribs etc.

2.5 Research Methodology

The Methodology employed to achieve the objectives of the thesis.

- Study of metals and polymers is to identify the best suitable polymer for design a lightweight, tough and durable hopper.
- DCPD material testing for ensuring quality & performance.
- Theoretical calculation of hopper parameters.
- Modelling of the hopper with Creo parametric according to dimensions of the vehicle loading platform and market requirement.
- Modal and Stress analysis of the model in MSC Nastran software. The zones cross the maximum stress value are redesign and then again analysed.
- Proto-building and assembly of the hopper on the vehicle with suitable supporting structure & adhesive joining for reducing vibration and stresses.

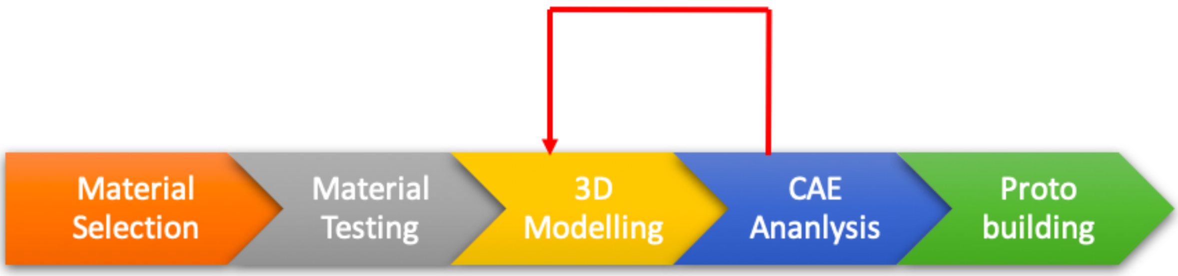

Figure 2. 4: Process work flow of DCPD hopper.

Chapter 3: MANFACTURING PROCESS OF HOPPER

3.1 Reaction Injection Moulding Process for DCPD

Reaction Injection Molding (RIM) was established by Dr. Bayer in 1969. In this manufacturing process, a chemical reaction between two monomers takes place to form a physical solid component and is different from the conventional shaping processes. RIM is also a bit separate process compared to the traditional thermoplastic injection moulding (TIM). In TIM, where cooling of the mould forms a Solid part within the mould cavity. RIM process two separate monomers to form a rugged plastic component.

Reaction injection moulding and injection moulding have nearly a similar name, so even experienced specialists and creators may think they are equivalent. Be that as it may, "Response" flags a major distinction – not at all like Reaction injection, RIM strategies use low-consistency liquid polymers in thermoset – not thermoplastic – forms. Through an assortment of synthetic responses, these polymers extend, thickens and solidify simply into the warmed shape after the chemical reaction thereby, substantially into more mind-boggling structures than formed by a standard reaction injection process. Polymer materials and trim systems can be selected and even modified to unequivocally convey wanted weight, quality, thickness and hardness attributes. The outcome is substantial polyurethane parts with a lot of lighter load than those made by progressively ordinary procedures.

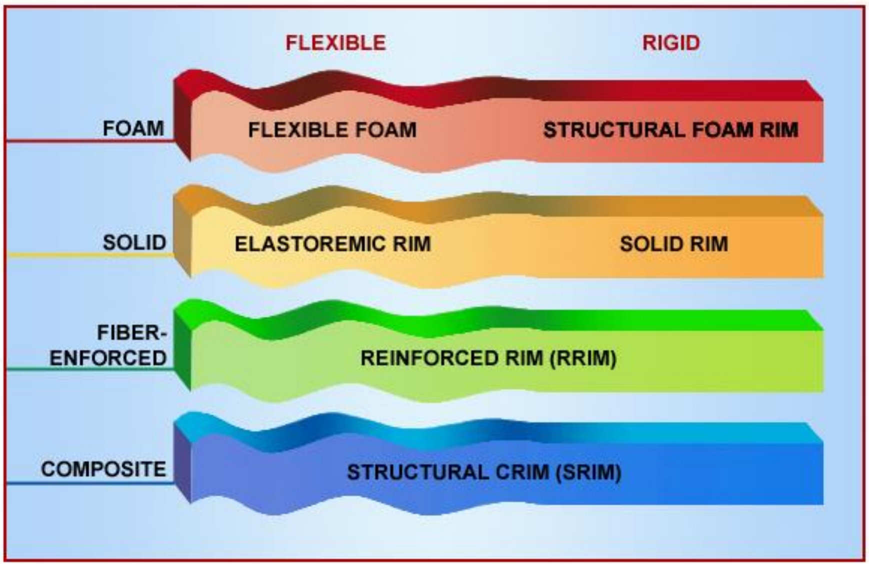

Figure 3.1: Different process of Reaction injection molding *(RIM1)***.**

Since these liquid polymers require less pressure (~1 bar) and lower temperatures (~90°) than run of the mill fixings, they can be infused into cost-productive aluminum moulds, and wooden mould (for proto building) thereby bringing down the tooling cost. The moulds are modestly warmed (~190°), yet the subsequent exothermic response rapidly brings the materials to (~325°) and speedily fixes the part inside the shape [12]. Fix times shift from not exactly a moment to a few minutes, contingent upon the part's size, geometry, capacity and divider thickness. Polymers and procedures can be picked to create strong, elastomeric, unbending froth, or adaptable froth completed polyurethane parts.

The RIM manufacturing process starts with polymer liquids (polyol and isocyanate) put away in extensive capacity tanks and administered by vast, heavy duty high pressure pumps. The polymers are recycled from the reservoirs to a multi-stream blend head on the machined aluminum or wax shape and back to the reservoirs in a consistent circle, as shown in Fig3.2.

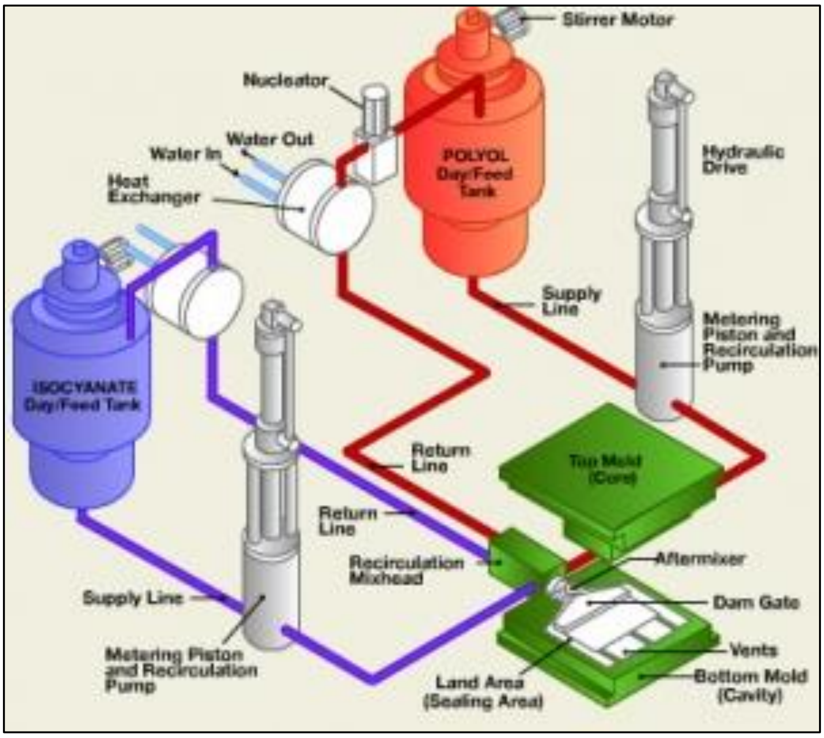

Figure 3.2: Systematic Diagram of Reaction injection process *(RIM1)***.**

At the point when each part is built, a cylinder or plunger inside the blending head withdraws, breaking the consistent circle, and the polymers at that point blend or encroach at a high pressure – around 80 bar – to guarantee the best possible blend of the polymers. The subsequent polyurethane enters the form through the after-blender, which keeps up the blend's properties while decreasing its speed to 6 – 7 bar.

Thermoset DCPD RIM (Reaction Injection Molding) includes a closed device, low PPM moisture and low PPM oxygen condition, as shown in Fig 2. It is similar to a reaction injection process but with an exception of thermosetting polymers being utilized (dicyclopentadiene), which requires relieving in the shape. In the event that fortifying specialists (generally glass strands or mica) are included, at that point the procedure is called reinforced reaction injection moulding (RRIM).

Reaction injection moulding offers critical focal points over injection moulding, yet in addition vacuum-framing, weight framing and cast forming.

A major portion of the reaction injection moulding process acts as a high-pressure pump. This process is suitable for thermosetting resin where a curing reaction takes place within the mould cavity. Reaction ingredients such as isocyanates, polyol, and polyamide do fast polymerization process & cycle time of the process is reduced & production rate is substantially enhanced.

DCPD RIM can create solid, adaptable, lightweight parts that could be effectively painted. The bi-part blend infused into the shape has a much lower consistency than a molted thermoplastic polymer, thusly huge, light-weight and slim walled things can be effectively delivered with DCPD RIM.

Basic things made with the DCPD RIM incorporates mudguards, fender and bumpers. Obliges exceptionally dimensional parts with a scope of part thicknesses. Amazingly shaped surfaces reasonable for Class A painted completion, great bond. Lightweight, sway safe parts with fantastic firmness and physical properties.

Effectively machined.

Completed parts will have a high impact strength and toughness.

In view of volume, tooling can be epoxy, wood (proto building), aluminum.

Figure 3.3: Actual mould core and cavity of RIM machine *(Schwartz, 2018)*.

Table 3.1 gives the basic differences in parameters of the components manufactured by RIM and TIM processes. The main varying parameters involve mould temperatures, injection temperatures, viscosity, injection pressure and clamping force.

Table 3.1: Difference between the parameters of RIM and TIM process [13].

Parameters	**TIM**	**RIM**
Mould temperature (°C)	25	70
Injection temperature (°C)	180-350	40
Viscosity (Pa.s)	100	0.1-1
Injection pressure (MPa)	1.5-40	0.1
Clamping force (ton/m2)	150-4000	50

It is clear from table 1. RIM requires higher mould temperature and lower injection temperature compared to TIM. Injection pressure and clamping forced require lesser than TIM process. The viscosity of fluid in RIM is very less compare to TIM because of TIM polymer pellet is melted than injected and in RIM liquid monomers injected in moulding.

Besides the development and growth of RIM technology have traditionally been associated with PU, other non-urethane chemical materials such as polyurethane, nylon, DCPD, EP and unsaturated polyester, have also been tried on this technology. For instance, nylon rim presented slow but steady progress during the last decade. It consists of copolymerization of nylon with an elastomer with different ratio values depending on the final use of the parts. Such combination allows reducing the viscosity of the material during the injection and the processing cost. This technology presents a good ratio of stiffness and toughness. The resistance to fatigue and abrasion is also good, as well as resistance to chemical compounds except to concentrate acids. In early 90s DSM tried this application of the automotive exterior body panels but without success, once this technology presents higher costs than other RIM technology. Nylon nowadays is mostly used in technical components and accounts for a presence of only 15 to 25kg per car [14].

Arising in 1980, dicyclopentadiene (DCPD) is a liquid engineered resin developed especially for reaction injection moulding (RIM), structural RIM (SRIM), RTM, near shape casting and rotational moulding. DCPD is a di-olefin monomer found in the off streams of petrochemical refineries used as a chemical intermediate for both flame retardants, EPDM elastomers and added to unsaturated polyester resin systems to enhance thermal stability. Dicyclopentadiene can be cracked into the monomer cyclopentadiene (C_5H_6) via thermal cracking and exists on two stereoisomers forms, the expo and endow isomers, being this last, the most common product sold as C 10 DCPD 12 (4,7·methano-3a,4,7,7a-tetrahydroindene) [15].

The DCPD polymerization is built on metathesis chemistry and occurs to Ring Opening Metathesis Polymerization (ROMP). A more detailed description can be found elsewhere and its molecular transformation process illustration can be viewed in Figure 3.4. The polymerization results in a crosslinking process (three-dimensional network structure) due to its highly exothermic reaction which starts from 40/60ºC till 150ºC. This reaction is promoted by various complexes of Tungsten and Molybdenum in conjunction with organo-metallic compounds of Al, Tin or Zinc. Other catalysts, such as Grubbs catalysts (based on transition metal) made the DCPD polymerization more robust and reduces also its odour. The combination of those components could be set in order to control the viscosity (which may vary from 170 to 330Cp), impact properties (which may vary from 4 to 4.6 J/cm) and its cycle time (which may vary from 4 to 10min). The material is self-released, not requiring any releasing agents and its post-cure are also unnecessary.

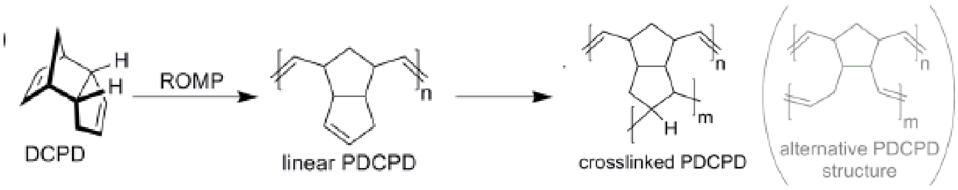

Figure 3.4: Ring Opening Metathesis Polymerization of DCPD *(Camboa, 2016)***[16].**

DCPD colour varies from no colour to turn on yellow or orange depending on catalysts used and curing temperature. During the polymerization, an approximately 6% reduction in the volume of the liquid material happens as it solidifies into the mould. The average shrinkage is around 1%, both parallel and perpendicular to the flow path. Part shrinkage depends on the part thickness and can be checked by process parameters, wall thicknesses variation and part design. A minimum amount of material has to be injected in order to promote a proper reaction and a minimum thickness of 3mm is advised. This material ensures low density (1030 Kg/) and a huge economic potential for low production volumes. Besides that, DCPD presents good mechanical properties even at cryogenic temperatures, among them good impact resistance, good corrosion and chemical resistance even at extreme temperatures (from -40°C to +160°C), as well as fracture toughness.

3.2 Adhesive bonding

The Adhesive bond is used to joining of DCPD to DCPD and metal supporting structure. Joining is also done by fasteners but due to notch sensitivity at the drill hole area cause failure. To improve strength, noise and vibration in structure suitable adhesive applied at the contact area of two parts. Polyurethane adhesive is good choice compare to epoxy because of its these good properties.

- Damping property
- Chemical resistant
- Service temperature (-40 to 90°C)
- Low shrinkage (2.5%)
- Elongation at break

Epoxy base adhesives are brittle and tend to break (loading or impact) without any warning. Moisture Curing mechanism of PU takes more than 4-5 days for full strength bonding. A Surface prepared by Sikaflex primer to make bonding strong and long-lasting.

Figure 3.5: Sikaflex 260IA adhesive cartage *(Ochoa, 2019)***.**

Chapter 4: DESIGN & MATERIAL TESTING

4.1 Part Design

Design a part in modelling software with the consideration of manufacturing constraints in order to avoid any issue during manufacturing. I design of DCPD hopper part in pieces because mould size is big which will not be moulded in a single cavity. Investment cost of the product is higher for big size tooling. While designing the mould part following factor have been considered.

4.1.1 Visible Surface Considerations

The design consideration a few points of interest in the DCPD RIM-process influencing the quality of the design part surfaces. It is expected to be remembered that the higher quality surface is acquired on the more sweltering piece of the shape. For parts like form panels, one typically thinks about a noticeable external surface (A-surface) and an inward/back surface (B-surface) of the part, with higher surface quality prerequisites to the external side. When in doubt, this is the pit side of the shape. The surface shaped by the centre of the instrument would arise out of lower quality.

4.1.2 Thickness

Thickness of the mould part is very crucial for injection moulding high thickness part require more cooling time, polymers are a bad conductor of heat. Thickness in range of 3-5 mm is preferred for the injection moulding process.

Uniform wall

Parts with uniform wall allow easy flow of monomer in a cavity with less restriction in flow. Uniform cooling and easy dispatching of product from the cavity without defected piece. The smooth surface of design tends to less stress concentration and thermal stress in part will be overcome by uniform wall thickness.

4.1.3 Polymerization shrinkage

Shrinkage of a part in the polymerization process is physical phenomena of linear shrinkage due to molecular chains and comparative speed of polymerization in different direction significantly analysed by the weight of reacting material and temperature profile.

Around 1% straight from shrinkage can be expected in parallel and perpendicular to the stream bearing. The heft of the volume change experiences the thickness, for example, perpendicular to the surface plane.

Shrinkage in part is mainly due to thermal shrinkage when a part gets cooled and molecular chain gets contracted. The Rapid change in thickness in part, by introducing ribs, fasteners holes and 90 angles bend profile reduces aesthetic and strengthen quality of product by shrinkage.

The method should be followed by designer to reduce effect of shrink marks fig 4.1.

- Design additional geometry to cover probable shrink marks.
- Sudden thickness increase areas would be smooth alterations.
- Provide thickness change line upper/below geometry to part.

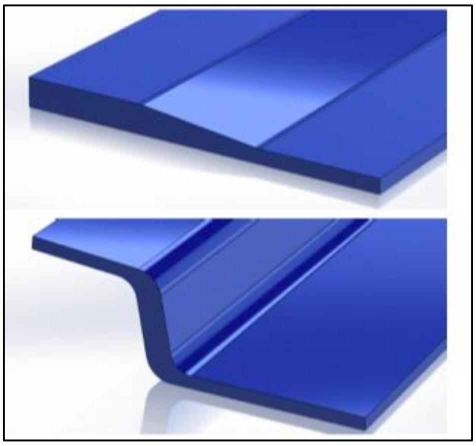

Figure 4.1: Shrink mark hiding design.

4.2 Ribs Design

Ribs (are often used to harden the part without essentially trading off its weight when contrasted with skin thickening. The disadvantages inborn to ribs are shriveled marks, challenges in shape filling and part demoulding.

Rib to surface thickness proportion of 0.6 connected to the plan fundamentally diminishes the shrink mark, in spite of the fact that this can’t ensure disposal of the issue. For non-stylish parts, the rib can be fixed as thick as the surface of the board, and significantly thicker. The typical routine with regards to covering up of shrink marks behind/under part’s regular (or uncommon) structure highlights.

To prevent rib filling issues,

- Orientation of ribs will be parallel to estimated direction of liquid flow in mould.
- Chamfers and fillet should be provided to connect ribs to surface panel properly.
- For escaping of air a big size reservoir provided.

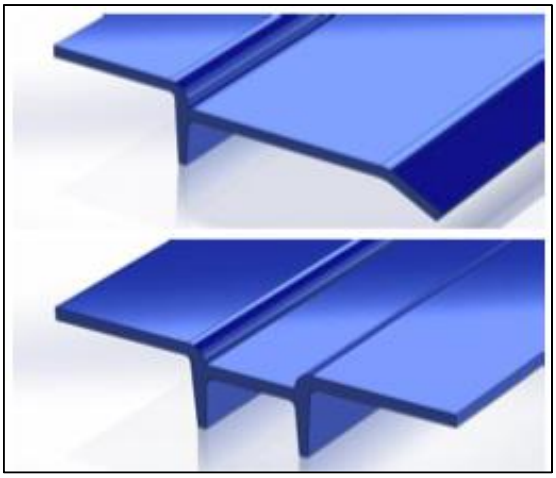

Figure 4.2: Single-directional Ribs.

4.2.1 Single-directional Ribs

A replacement of metal sheet with polymer with same straight/equivalent stiffness to get light weight benefits. Following equation is used,

$$\text{Em x Tm}^3 = \text{Ep x Tp}^3 \quad \textbf{(4. 1)}$$

Em = Young's Modulus of metal (Mpa)

Tm = Thickness of metal sheet (mm)

Ep = Young's Modulus of polymer (Mpa)

Tp = Thickness of polymer sheet (mm)

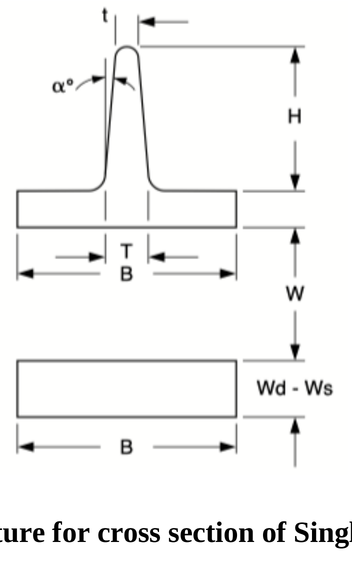

Figure 4.3: Nomenclature for cross section of Single-directional ribbing.

$$t = T - 2H\ tan\alpha \quad (4.\ 2)$$

$$A\ (Area) =\ BW + \frac{H(T+t)}{2} \quad (4.\ 3)$$

W_d = Equivalent thickness for deflection

W_s = Equivalent thickness for stress

Ribs and strength supporting member minimum thickness of $^1/_2 - ^2/_3$ times as the base sheet and $\alpha = ^1/_4 - ^1/_2\,^\circ$ draft is provided in support member and ribs for easy dispatch from mould cavity. The aim of using less thickness in ribs compare to base to reduce shrink marks on outer surface to maintain aesthetic look. Distortion in part will occur if we don't provide proper draft angle in ribs during dispatching.

The whole structure to define one of the smaller sections, the equivalent breadth BEQ is used.

$$BEQ = \frac{total\ breadth\ of\ section}{number\ of\ ribs} = \frac{B}{N} \quad (4.\ 4)$$

By using moment of inertia and Section modulus equation for ribbed zone, wall thickness ratios calculated and plotted in a graph. These calculations are based on 40% reduction in rib thickness of sheet thickness.

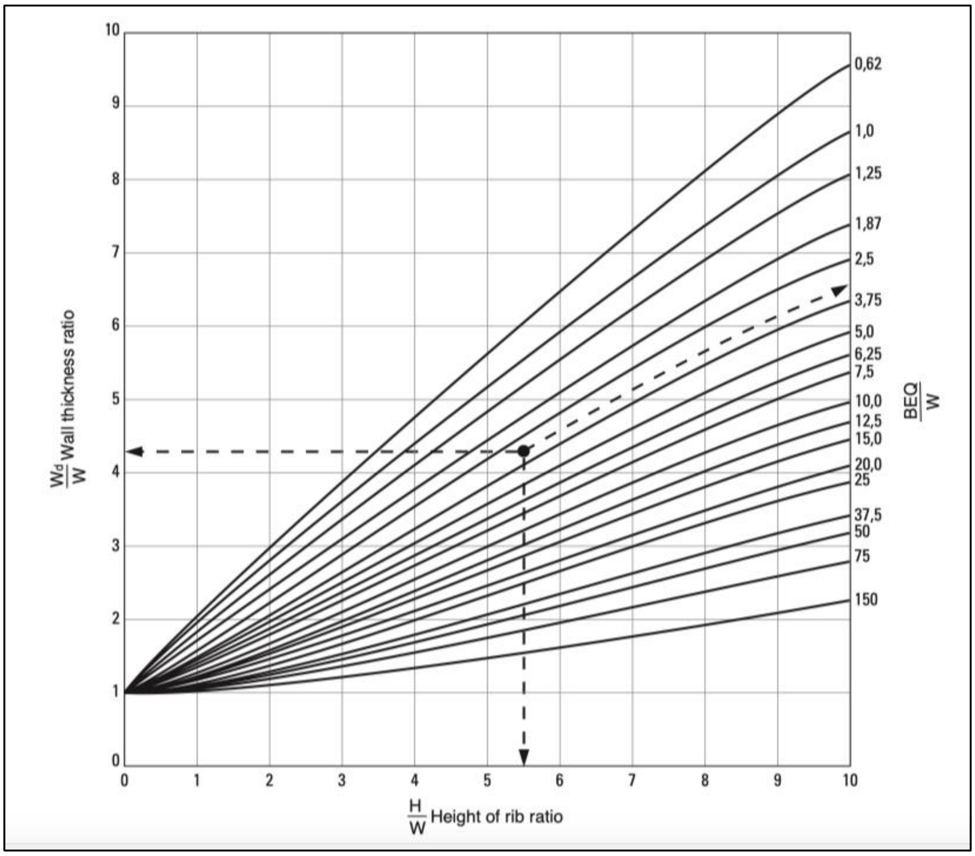

Figure 4.4:Deflection curves based on moment of inertia, the computer programmed curves in this graph *(Pont)***[17].**

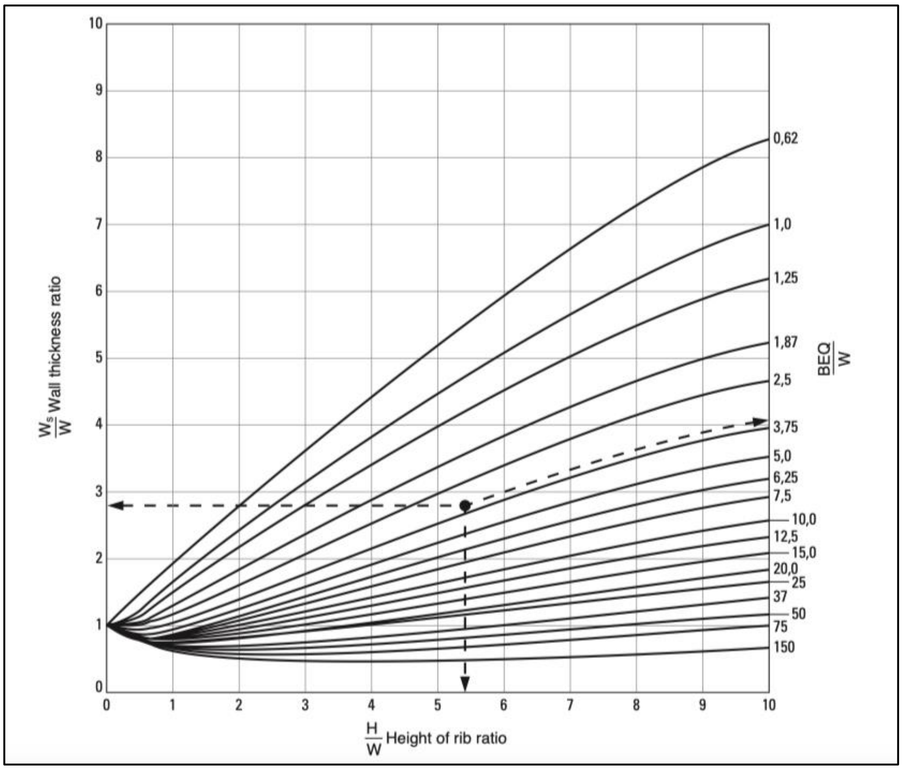

Figure 4.5: Stress curves based on section modulus, the computer programmed curves in this graph ***(Pont)*** **[17].**

With the help of deflection and stress curve, we are able to decide equivalent deflection thickness to calculate the moment of inertia of rib and further we find the deflection of ribs at a certain load. By equivalent stress thickness to calculate section modulus of rib and further find stress in ribs as applied load.

Alternative method of molding a single –piece part with ribs, when shrink marks are more to overcome its. This part is additionally manufactured and assembled by using adhesive bond with suitable adhesive. Metal reinforced element also used in this "Hat-shape profile" fig 4.6 to provide strength to part.

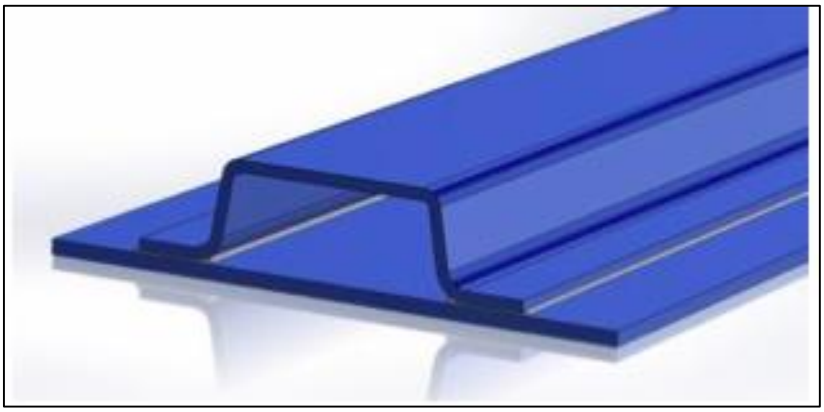

Figure 4.6: Hat shape Ribs.

4.2.2 Fillet and Radii

Liberal filets and corner radii are suggested. Sharp corners ought to be evaded as they can trap bubbles and make pressure focuses. In this way, it is prescribed to apply no less than a 1.5mm span filet to outside and inside corners of a section structure. 2 to 3mm span filets are explicitly suggested for corners contradicting the separating line fig 4.7.

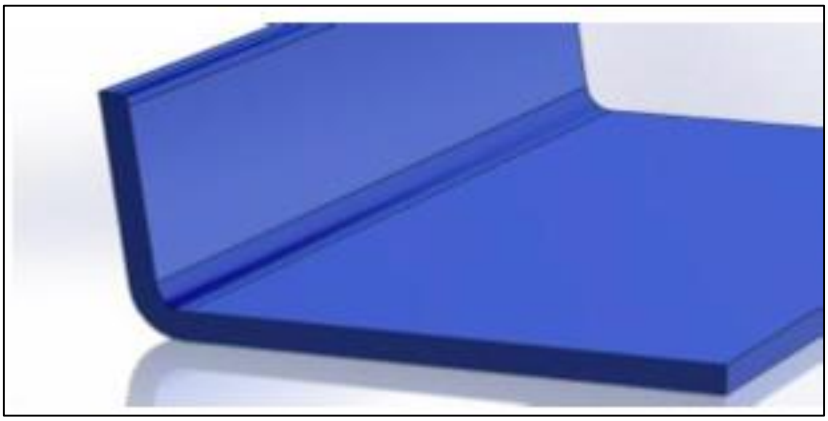

Figure 4.7: Fillet and radii at corner.

4.3 End Life Evaluation

To concoct environmental studies, for example, those expressed beforehand, an End Life of Vehicles (ELVs) was assembled. ELVs is a technique to represent the ecological effects related with an item or an administration from its origins as far as possible of life. As per ISO 14001 an ELVs can be partitioned into three principle stages:

a) Production phase, the energy requirements for completing primary and secondary materials processes for manufacturing them into a finished product.
b) Uses phase, including the energy over the entire lifetime of the product fulfill their function.
c) End-of-life phase, the energy required to disposal of the scrap product and whatever energy is consumed in its recycling.

In other words, it takes into account all energy and material flows through the production, use and end of life with aim of identify the sources that most contribute for the environment impact. An ELVs may have different outputs types, being CO 2 emissions and energy consumption the most common. Vehicle end of life is currently used in the automotive industry too, in order to measure the energy required during the complete life of a car. The automotive ELVs model can be summarized into four main stages: raw material processing, production, operating and recover, as can be seen through Figure 4.8.

4.3.1 End Life Evaluation equations

For this particular work, just energy was estimated, since the CO2 emanations may shift from energy source and its very own effectiveness. Therefore, the complete energy required for the existence cycle of the hopper bin is gotten careful an aggregate of the energy required over the four phases exhibited previously.

$$Energy_{Total} = Energy_{Material\ Refining} + Energy_{Production} + Energy_{Operated} + Energy_{Recycling} \quad (4.\ 5)$$

where,

$Energy_{Material}$, refining, is the energy needed to process the material from raw, including extraction.

$Energy_{Production}$, is the energy needed for the manufacturing of a design part.

$Energy_{use}$, is the energy consumed during its operation use.

$Energy_{Recycling}$, is the energy spent or gained from the recycling process. At the end of a product life, several recycling strategies are available, among them reuse, recycling, down cycling, combustion (for energy recovery) and landfill. For all types, energy spent/recovered from recycling can be achieved through equation.

$$Energy_{Recycling} = Energy_{Scrap} + Energy_{End\ of\ Life} \quad (4.\ 6)$$

$Energy_{Scrap}$, is the power required for segregating and collection of scrap part. Its depends on type of material, process may be one collection and two segregating stages. For collection, primary and secondary sorting energy calculation, factors of 0.2, 0.3 and 0.5 are respectively attributed. Thus, the total disposal energy is obtained by multiplying the mass of the part/material by the factor in which is being processed. For parts/materials being landfilled, the $Energy_{Recycling}$required = $Energy_{Scrap}$, since no additional segregating stages are necessary.

$Energy_{End\ of\ Life}$,is the end of life of the part or material? For instance, after collection and sorting phases, parts or materials might be down cycled and reintroduced in the life chain with inferior quality or incinerated in order to allow recovering energy from them. For down cycle and heat recovery, the following equations (4.5) and (4.6) shall be adopted, respectively:

$$Energy_{End\ of\ Life} = \beta \times (Energy_{Recycling} - Energy_{Embodied\ Material}) \times Mass \quad (4.\ 7)$$

where,

β, is the nominal down cycle factor, as 0.5 for metals and 0.2 for plastics

$Energy$ is the energy required on recycling,

$Recycling\ Energy$ is the energy embodied on the material,

$Embodiedmaterial\ Mass$, is the mass of part.

$$Energy\ Incineration\ = -H\ Combustion \times Mass \times Efficiency\ Combustion \quad (4.\ 8)$$

where,

$-H\ Combustion$, is the material heat energy (MJ/kg),

$Mass$, is the mass of part,

$Efficiency$ combustion, is the combustion efficiency (0.25)

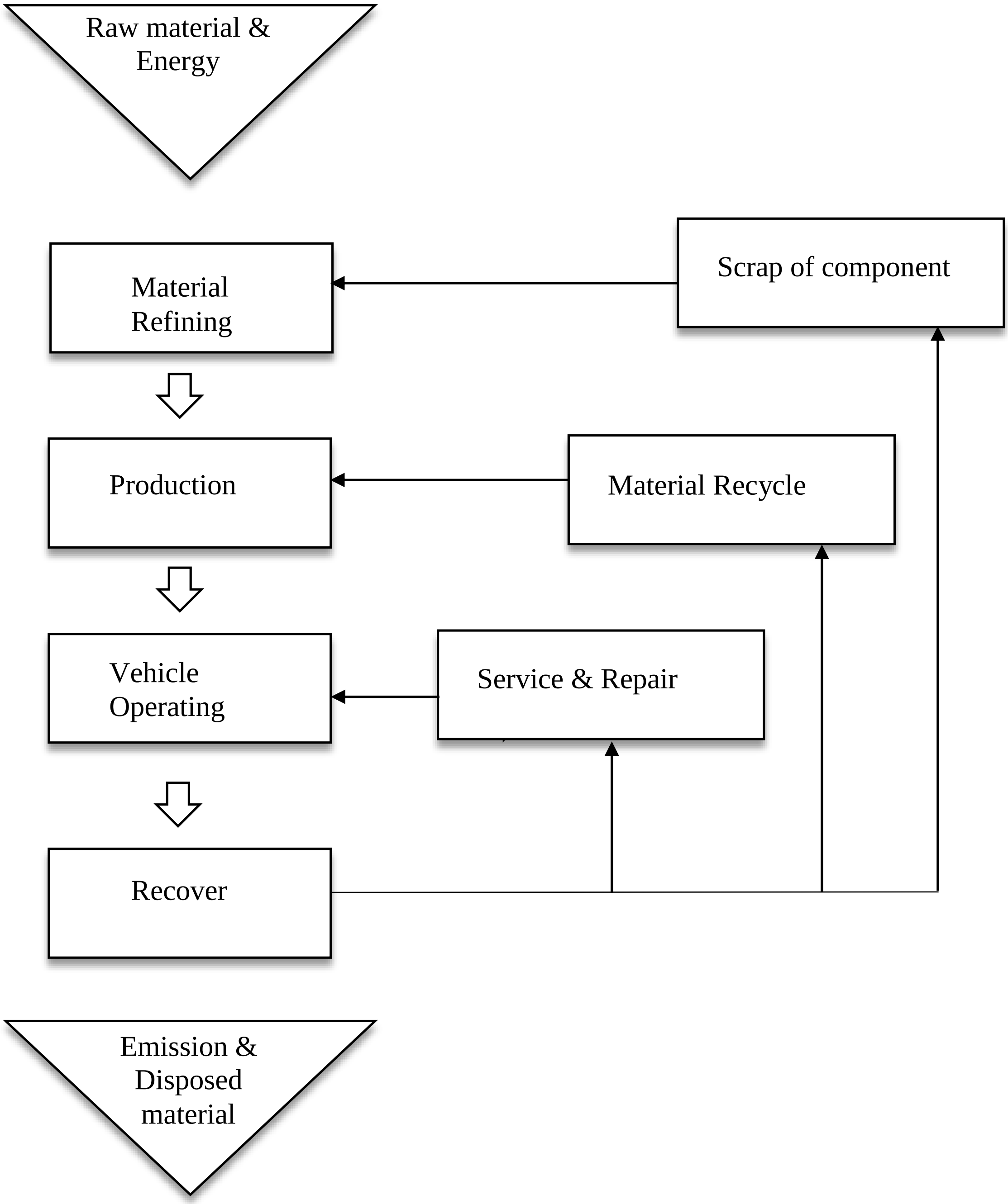

Figure 4.8: Life Cycle Flow Diagram of Vehicle component [18].

4.4 Material Testing of DCPD

Physical and Mechanical property of DCPD material according to Telene 1650A/BK test. However, due to some process ability variations and uncertainty, these values were reviewed by recurring to DCPD samples testing.

Table 4.1: DCPD Property data sheet *(Telene, 2015)*.

Properties	Standard	SI Unit	Value
Specific Gravity	ISO 1183		1.03
Tensile Modulus	ISO 527	MPa	1870
Tensile Strength @ yield	ISO 527	MPa	43
Elongation @ Yield	ISO 527	%	5
Flexural Strength	ISO 178	MPa	67
Flexural Modulus	ISO 178	MPa	1850
Compressive Strength	ISO 604	MPa	70
Shear Strength	ASTM D732	MPa	53
Impact Strength	ISO 180	KJ/m2	30
Rockwell Hardness	ISO 2039-2	HRR	114
Heat Distortion Temperature	ISO 75	°C	120
Linear Thermal Expansion	ISO 11359	m/m/°C	79 x 10-6

Ultimate tensile test

To validate the DCPD material quality, a tensile strength test is carried out according to standard (ASTM D638) in TATA Motors metrology department. Six specimens were machined from DCPD sheet according to TS5454. Shape of specimen in dog bone shapes and narrows width of 13mm.

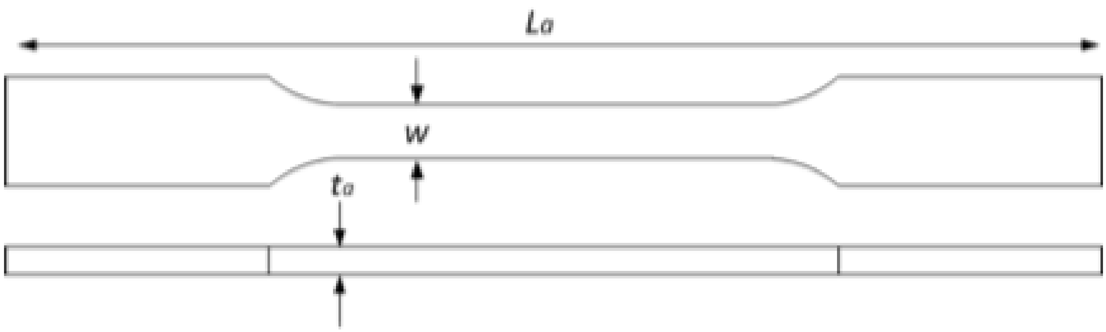

Figure 4.9: Drawing of Specimen for tensile strength test accordance to standard.

Specimen is held between jaws of Universal Tensile Machine by star tensile machine, load cell of 5000Kg. A 70mm extensometer was applied and test speed is set to 5mm/min. The tensile test specimen was placed in the machine jaw with 100mm distance between grips.

Figure 4.10: Specimen for Tensile Test.

Table 4.2: Specimens Test Results.

Specimens	Thickness	Width	σ max	E
	(mm)	(mm)	(MPa)	(MPa)
1	7.5	13.1	43.45	2010
2	7.46	13.02	44.23	1920
3	7.45	13.07	41.5	1870
4	7.46	13.05	44.2	1940
5	7.47	13.2	43.6	1980
6	7.48	13.05	43.1	1890
Average	7.47	13.08	43.34	1935

A mean value of 43.34 MPa and 1935 MPa was found for maximum tensile strength and Tensile modulus respectively, which are slightly more than that to define by telene standard. Poisson's ratio was not measured because of unavailability of strain gauge for measuring strain rate. Material is accepted to achieve a standard value. These test result values are used in finite element Analysis of model.

Hardness Test

Shore D Hardness is conducted on DCPD material specimen of 50X50 mm dimension. Shore D test is specially designed test for polymer, elastomer and rubber. It is a measure of the resistance of a material to penetration of sharp needle indenter which is spring loaded.

Table 4.3: Shore D test results on Painted surface of DCPD.

Test	1	2	3	4	5	6	7	Mode
Shore D	84	83	83	82	85	82	82	82

Table 4.4: Shore D test results on non-Painted surface of DCPD.

Test	1	2	3	4	5	6	7	Mode
Shore D	76	77	76	77	77	78	77	77

Figure 4.11: Hardness Tester.

The hardness of material is greater when we do on painted surface actually we are using DCPD material painted in Hopper proto. Paint gives more resistance to penetration or abrasion according to shore D test. DCPD show excellent hardness compares to other polymers of their class.

Flexural Strength test

A three-point bending test performs to examine the flexural strength of DCPD polymer.

A rectangular bar set between two cylindrical supports rods and is charged by means of a loading nose midway between the loading span. The specimen is deforming until rupture in the outer surface of the specimen. The test speed is set to 1mm/s to measure a precise value of a specimen.

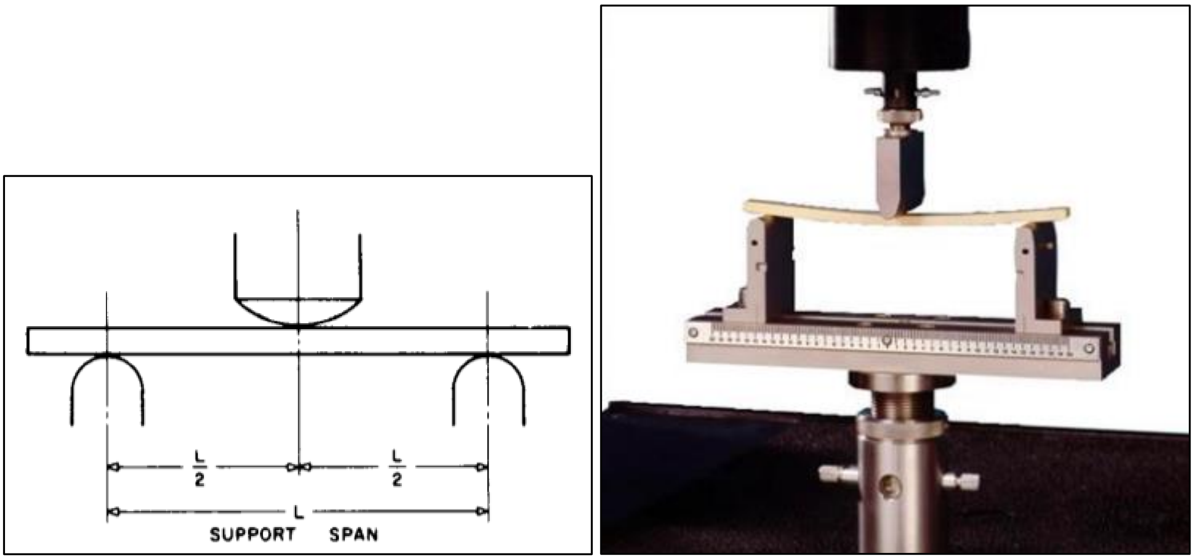

Figure 4.12: Three-point bending test setup (D790, 2003)**.**

Flexural Stress

$$\sigma_f = \frac{3PL}{2bd^2} \quad (4.9)$$

where,

σ = stress in the outer fibers at centre of specimen (MPa)

P = load at applied at the given point (N)

L = support length (mm)

b = width of specimen (mm)

d = depth of specimen (mm)

Flexural Strain

Nominal fractional change in the length of an element of the outer surface of the test specimen at centre, where the maximum strain appears. It may be calculated for any deflection point.

$$\in_f = \frac{6Dd}{L^2} \quad \textbf{(4. 10)}$$

Where,

$\in_f$ = strain in the outer surface (mm/mm)

L = support length (mm)

d = depth of specimen (mm)

D = maximum deflection at the mid of the specimen (mm)

Modulus of Elasticity

Tangent modulus of elasticity

$$E_B = \frac{L^3 m}{4bd^3} \quad \textbf{(4. 11)}$$

Where,

E_B = elastic modulus in bending condition (MPa)

L = support length (mm)

b = width of specimen (mm)

d = depth of specimen (mm)

m = slope of the tangent to the initial straight-line of the load-deflection curve (N/mm)

Chord Modulus

$$E_f = \frac{(\sigma_{f2} - \sigma_{f1})}{(\in_{f2} - \in_{f1})} \quad \textbf{(4. 12)}$$

Where,

σ_{f2} & σ_{f1} = Flexural stress at two discrete points.

$\in_{f2}$ & $\in_{f1}$ = Flexural strain at two discrete points.

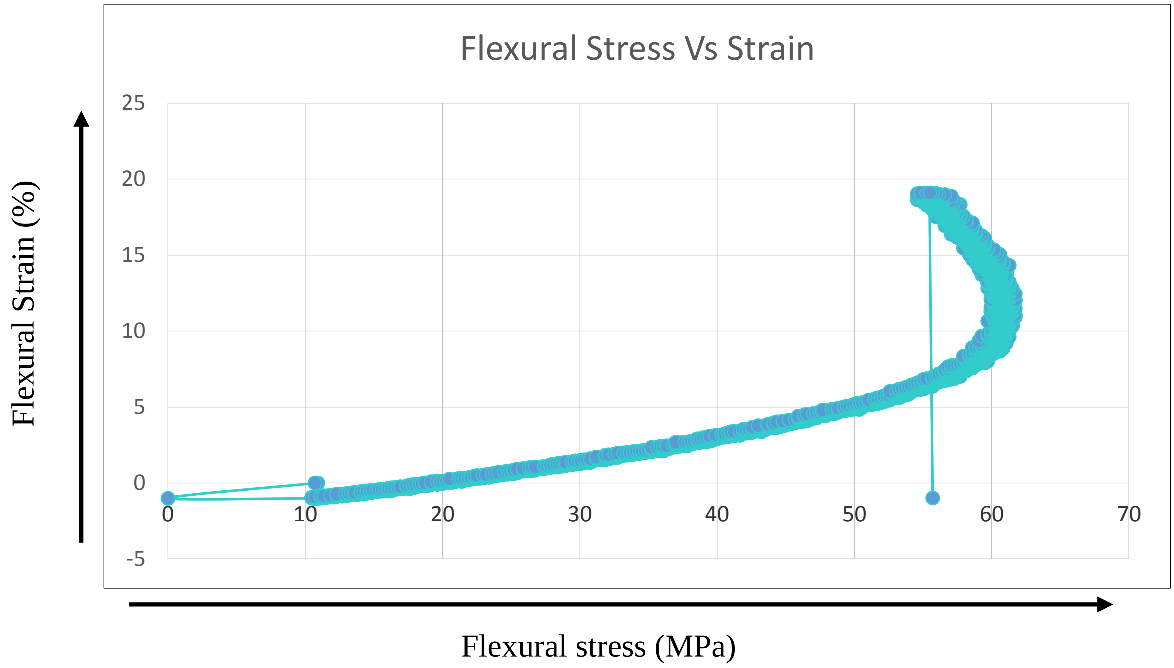

Figure 4.13: Flexural Stress Vs Flexural Strain.

Three-point bending test shows the maximum flexural strength of 61.7MPa, which is less than the standard value of flexural strength (67MPa). Moulding defects are detected in a sample piece when a camera view of DCPD.

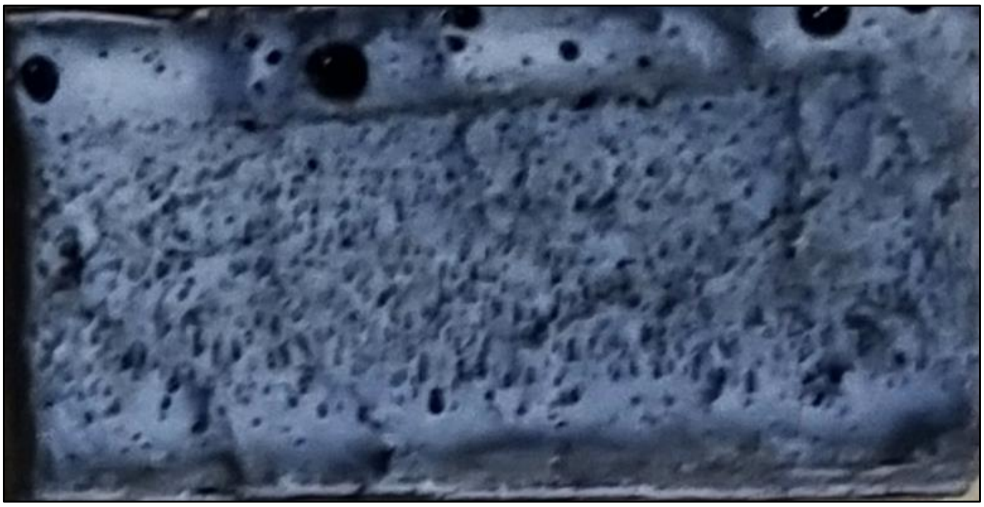

Figure 4.14: Camera image of DCPD material after fracture.

4.5 DCPD Chemical Resistance Non reinforced grade

The following table gives suggestions on the appropriateness of DCPD polymers in applications where the material comes into intimate & sustained contact with the liquid medium.

- For individual applications in specific chemical environments, testing prior to use is recommended.
- The chemical resistance at elevated temperatures in non-oxidative acid or alkaline media is excellent, as it is in weaker solutions of sulphuric & nitric acids at ambient temperatures.
- The table has been constructed by grouping the results of the following mechanical and physical tests and comparing to untreated polymer:
- Change in Ultimate tensile strength
- Change in yield strength
- Change in flexural modulus
- Change in shore D hardness
- Change in dimensions

✕ = Not Recommended
✓ = Recommended

Table 4. 5: Effect of different chemicals on DCPD material at 24°C, 65°C and 100°C temperature.

Temperature	24°C				65°C				100°C			
Duration	7d	30d	90d	180d	7d	30d	90d	180d	7d	30d	90d	180d
Reagent												
10% Acetic Acid	✓	✓	✓	✓	✓	✓	✓	✓	✓	✓	✓	✓
50% Phosphoric Acid	✓	✓	✓	✓	✓	✓	✓	✓	✓	✓	✓	✓
30% Phosphoric Acid	✓	✓	✓	✓	✓	✓	✓	✓	✓	✓	✓	✓
55% Phosphoric Acid	✓	✓	✓	✓	✓	✓	✓	✓	✓	✓	✓	✓
70% Phosphoric Acid	✓	✓	✓	✓	✓	✓	✓	✓	✓	✓	✓	✓

50% Potassium Hydroxide	✓	✓	✓	✓	✓	✓	✓	✓	✓	✓	✓	✓
13% Sodium Hypochlorite	✓	✓	✓	✓	✓	✓	✓	✓	✓	✓	✓	✓
30% Fluosilicic Acid	✓	✓	✓	✓	✓	✓	✓	✓	✓	✓	✓	✓
10% Hydrogen Peroxide	✗	✗	✗	✗	✗	✗	✗	✗	✗	✗	✗	✗

Temperature	24°C				65°C				100°C			
Duration	7d	30d	90d	180d	7d	30d	90d	180d	7d	30d	90d	180d
Reagent												
25% Sulphuric Acid	✓	✓	✓	✓	✓	✓	✓	✓	✓	✓	✓	✓
75% Sulfuric Acid	✓	✓	✓	✗	✗	✗	✗	✗	✗	✗	✗	✗
10% Nitric Acid	✓	✓	✓	✓	✓	✓	✗	✗	✗	✗	✗	✗
50% Nitric Acid	✓	✗	✗	✗	✗	✗	✗	✗	✗	✗	✗	✗
50% Hydrochloric Acid	✓	✓	✓	✓	✓	✓	✓	✓	✓	✓	✓	✓
30% Hydrochloric Hydroxide	✓	✓	✓	✓	✓	✓	✓	✓	✓	✓	✓	✓
10% Sodium Hydroxide	✓	✓	✓	✓	✓	✓	✓	✓	✓	✓	✓	✓
50% Sodium Acid	✓	✓	✓	✓	✓	✓	✓	✓	✓	✓	✓	✓
Water	✓	✓	✓	✓	✓	✓	✓	✓	✓	✓	✓	✓

Temperature	24°C				65°C				100°C			
Duration	7d	30d	90d	180d	7d	30d	90d	180d	7d	30d	90d	180d
Reagent												
30% Flu silicic Acid	✓	✓	✓	✓	✓	✓	✓	✓	✓	✓	✓	✓
Glycerol pure	✓	✓	✓	✓	✓	✓	✓	✓	✓	✓	✓	✓
20% Hydrofluoric Acid	✓	✓	✓	✓	✓	✓	✓	✓	✓	✓	✓	✓
Sulphur Dioxide SO_2	✓	✓	✓	✓	✓	✓	✓	✓	✓	✓	✓	✓

80% Lactic Acid	✓ ✓ ✓ ✓	✓ ✓ ✓ ✓	✓ ✓ ✓ ✓
30% Sodium Bisulfite	✓ ✓ ✓ ✓	✓ ✓ ✓ ✓	✓ ✓ ✓ ✓
Hydrogen Sulfide H_2S	✓ ✓ ✓ ✓	✓ ✓ ✓ ✓	✓ ✓ ✓ ✓
40% Dimethylamine	✓ ✓ ✓ ✓	Pressure vapour >3bar	Pressure vapour >10bar
32% Ammonium Hydroxide	✓ ✓ ✓ ✓	Pressure vapour >8bar	Pressure vapour >20bar

Source: TELENE SAS (Innovative chemistry for designers)

Chapter 5: THEORY OF DYNAMICS & STRENGTH

5.1 Introduction

Vibration develops in vehicle structure due to the presence of dynamic motion, i.e. tire bump and engine crank motion that vary in time (at a different speed or road condition). These motion introduce new difficulty compare to the static structure. When we study a static structure more load cause to deflection and more strength is therefore needed. The condition is not as insignificant when dynamic forces are subjected. In this situation, the magnitude of the force might not be significant as the frequency it is changing with. When excitation frequency reaches to natural frequency (Eigen frequency) of the structure, response of vibration too larger than force with same magnitude but different frequency.

5.2 Damping and vibration properties of DCPD polymer

Excessive vibration causes reduced efficiency of product, waste of energy and increase chances of fatigue failure of the structure. Hence, undesirable vibrations should be damped to increase product life. We use polymer material which having a higher damping coefficient than metal. Polymer reduced vibration and also noise whereas metal vibrates more and generate loud noise.

Vibration analysis of lightweight material requires because when mass is decreased, the frequency and hence the pitch increase. More vibration in the body causes fatigue failure, so the vibration of the vehicle should be under the limit standard.

In structural response can be represented by a Single degree of freedom (SDOF) model, we look at some aspects of SDOF dynamics. In hopper tipper, we examine the way in which SDOF structure can be modelled in physical, time and frequency domains. This model is not intended to represent physical structure, but serve an instrument for interpreting dynamic behavior.

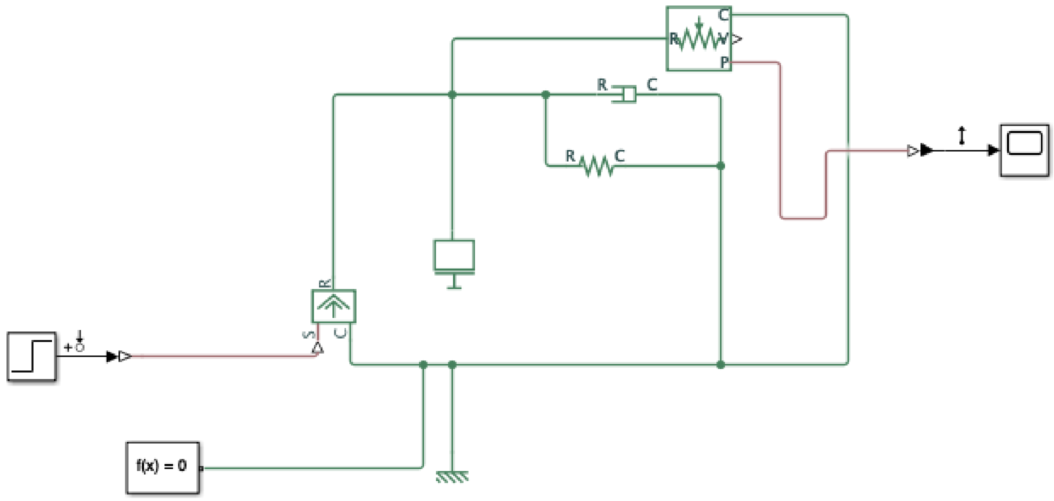

Figure 5.1: Systematic Diagram of Single degree of freedom vibration Simulink model in matlab.

Natural frequency of vibration in varying mass condition is calculated by:

$$\omega_n = \sqrt{\frac{3\,E\,I}{L^3\,M_i}} \tag{5. 1}$$

Natural time period of transverse direction is calculated by:

$$T_n = \frac{2\pi}{\omega_n} \tag{5. 2}$$

Damping coefficient

$$C = 2\,\xi\,\sqrt{kM} \tag{5. 3}$$

T_n = Time period of transverse direction (sec).

ω_n = Natural frequency of hopper (Hz)

ξ = Damping ratio

k = Stiffness (N/m)

M = Mass of structure (Kg)

Natural Time period denotes the time taken in completion of cycle of vibration.

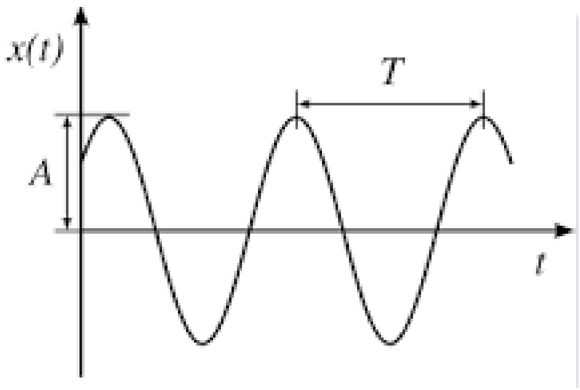

Figure 5.2: Period of Vibration.

5.3 Free-vibration Response in hopper due impact mass

A hopper is cantilever hinged at a point subjected to a uniform distributed load. An analysis of response vibration after hitting the floor of the hopper. We decide the velocity of hitting with reference to height of object release.

$V = \sqrt{2\,g\,h}$

g = acceleration due to gravity (9.81 m/s^2)

h = height of release.

V = Velocity at object hit the surface.

A mass m, release from height h strike the mass M of a damped single degree of freedom hopper shown in fig.5.3 (B). Displacement of structure due to mass hitting

$$X_e = \frac{m}{M+m}\sqrt{2gh} \qquad \textbf{(5. 4)}$$

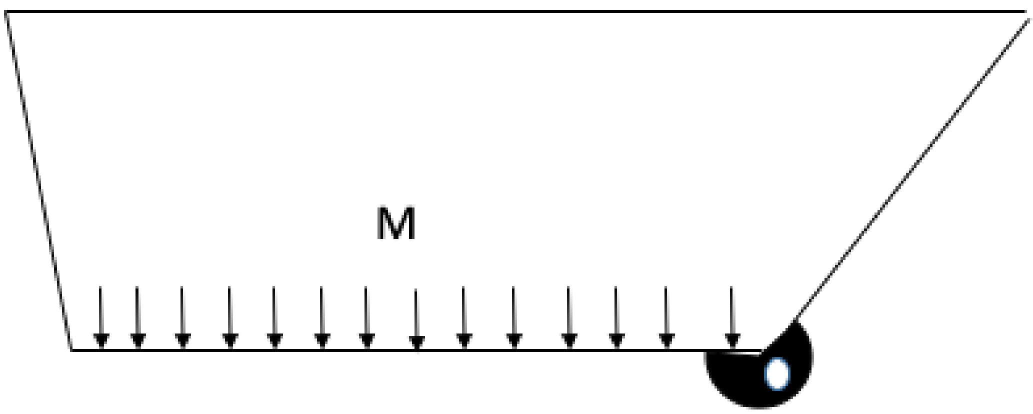

A)

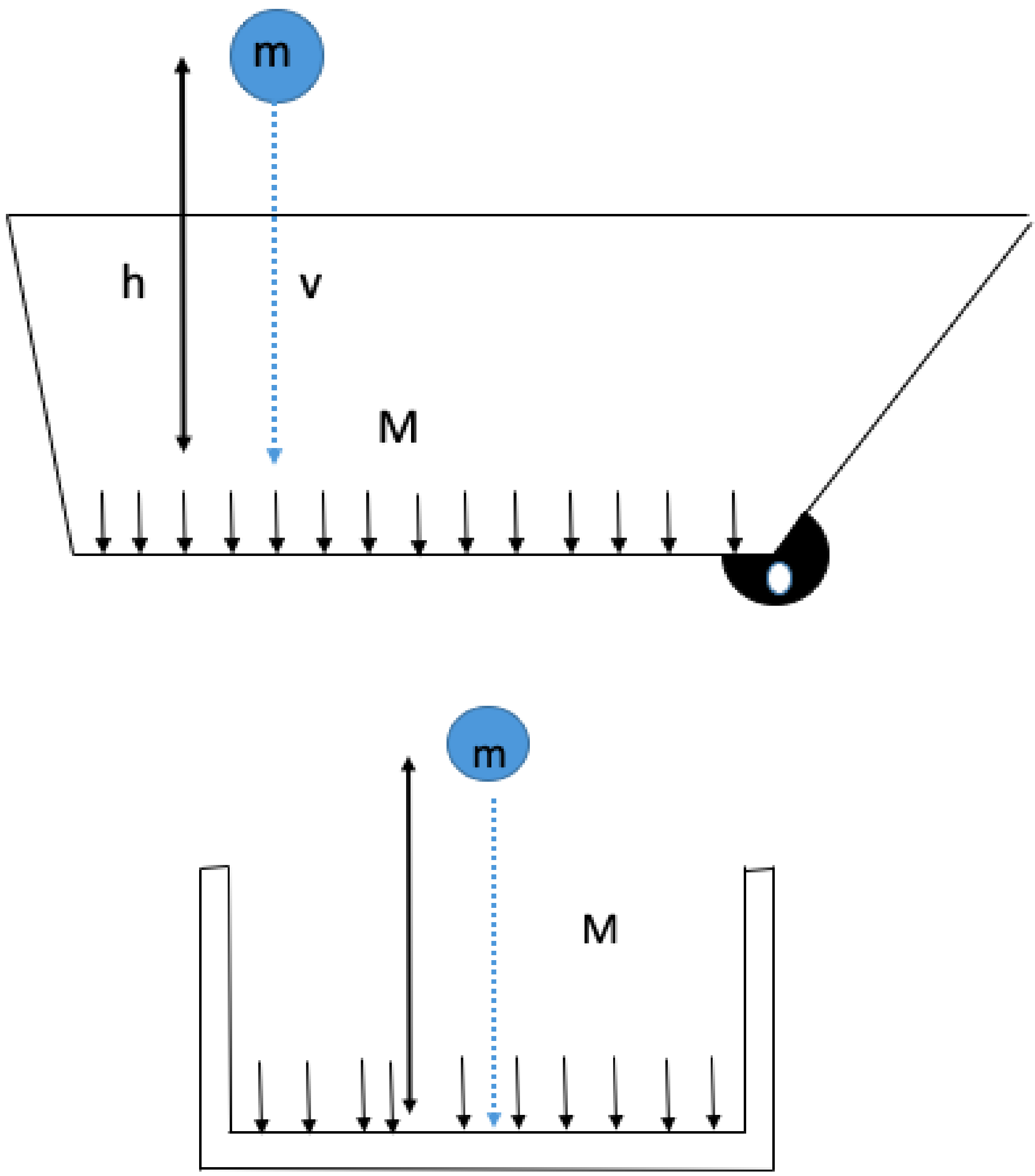

B)

Figure 5.3: Hopper tipper A) At UDL loading B) Hopper hit by a mass m.

5.4 Modal Frequency Analysis by Finite Element Method

Theoretical general equation for the calculation of modal vibration response in finite element. The mode shapes and the natural frequency of a hopper calculated because of many purposes. Primary purpose is to evaluate the dynamic interface between a different part and its supporting members. For example, hopper is mounted on the vehicle chassis where lots of vibration due to tire bump by rough roads and engine vibration transfer through chassis, to avoid resonance issue. Resonance vibration is highly dangerous to structure, failure chances for low vibration.

A special reduced form of the equation of motion required for the solution of the equation of motion at the natural frequency and normal modes. We consider there is no damping and loading condition on the hopper to reduce the equation of motion in matrix form.

$$\boldsymbol{M}(\ddot{u}) + \mathbf{K}(\mathbf{u}) = \mathbf{0} \qquad \textbf{(5. 5)}$$

Where

M = mass matrix

K = stiffness matrix

To solve the equation a harmonic solution:

$$\boldsymbol{u}(\boldsymbol{t}) = \boldsymbol{A}\boldsymbol{cos}(\boldsymbol{\omega t})\boldsymbol{\varphi} + \boldsymbol{B}\boldsymbol{sin}(\boldsymbol{\omega t}) \qquad \textbf{(5. 6)}$$

Where:

$\boldsymbol{\varphi}$ is the eigenvector

ω is the circular natural frequency

Sinusoidal form of the solution means that all the degrees-of-freedom of the vibrating structure move in a synchronous manner. The structural configuration does not change its basic shape during motion; only its amplitude changes. By using the harmonic solution to the differential equation, after simplifying it becomes:

$$[\boldsymbol{K} - \boldsymbol{\omega}^{\mathbf{2}}(\boldsymbol{M})]\ \boldsymbol{\varphi} = \mathbf{0} \qquad \textbf{(5. 7)}$$

This equation is called the Eigen equation, which is a set of homogeneous algebraic equations for the components of the eigenvector and forms the basis for the eigenvalue problem.

$$[\boldsymbol{A} - \boldsymbol{\lambda I}]\boldsymbol{x} = \mathbf{0}; \qquad \textbf{(5. 8)}$$

where:

A = Square matrix

λ = eigenvalues

I = Identity matrix

x = Eigen vector

There are two possible solution forms for this equation

1) If $\det[k] - \omega^2[M] \neq 0$, the only possible solution is

$$[\boldsymbol{\varphi}] = \mathbf{0}$$

This represents the case of no motion

2) If $\det[k] - \omega^2[M] = 0$, then a solution with $\boldsymbol{\varphi} \neq \mathbf{0}$ is obtained,

$\det[k] - \lambda^2[M] \neq 0$, where **λ = ω²**

The determinant is zero only at a set of discrete eigenvalues λ_i or ω_i.

$$\{[\boldsymbol{K}] - \boldsymbol{\omega}^2[\boldsymbol{M}]\}\boldsymbol{\varphi} = \mathbf{0}$$

There is an eigenvector which satisfies the equation above and corresponds to each eigenvalue, thus this equation can be rewritten as:

$$\{[\boldsymbol{K}] - \boldsymbol{\omega}_i^2[\boldsymbol{M}]\}\boldsymbol{\varphi}_i = \mathbf{0}, \ \mathbf{i = 1,2,3 \ldots}$$

Each eigenvalue and eigenvector define a free vibration mode of the structure. The i^{th} eigenvalue is related to the i^{th} natural frequency as follows:

$$\boldsymbol{f}_i = \frac{\boldsymbol{\omega}_i}{\mathbf{2}\boldsymbol{\pi}}$$

where:

f = Natural frequency

$\boldsymbol{\omega}_i = \sqrt{\boldsymbol{\lambda}_i}$

The number of eigenvalues and eigenvectors is equal to the number of degrees-of freedom that have mass or the number of dynamic degrees-of-freedom. There are a number of characteristics of natural frequencies and mode shapes that make them useful in various dynamic analyses. First, when a linear elastic structure is vibrating in free or forced vibration, its deflected shape at any given time is a linear combination of all of its normal modes:

$\{\boldsymbol{u}\} = \boldsymbol{\Sigma}_{i}(\boldsymbol{\varphi}_{i})\boldsymbol{\xi}_{i}$

where:

{u} = physical displacements vector

$(\boldsymbol{\varphi}_{i})$ = i^{th} mode shape

$\boldsymbol{\xi}_{i}$ = i^{th} displacement of modal

Second, if solution is symmetric and real:

$(\boldsymbol{\varphi}_{i})^{\boldsymbol{T}}[\boldsymbol{M}](\boldsymbol{\varphi}_{i}) = \mathbf{0}$ if □ $i \neq j$

$(\boldsymbol{\varphi}_{i})^{\boldsymbol{T}}[\boldsymbol{M}](\boldsymbol{\varphi}_{i}) = \boldsymbol{m}_{\boldsymbol{j}}$ = j^{th} generalized mass – (orthogonality property)

and

$(\boldsymbol{\varphi}_{i})^{\boldsymbol{T}}[\boldsymbol{M}](\boldsymbol{\varphi}_{i}) = \mathbf{0}$ if $i \neq j$

$\boldsymbol{(}(\boldsymbol{\varphi}_{i})^{\boldsymbol{T}}[\boldsymbol{M}](\boldsymbol{\varphi}_{i}) = \boldsymbol{K}_{\boldsymbol{j}}$ = j^{th} generalized stiffness = $\omega^2 m_j$ (orthogonality property)

$$\boldsymbol{\omega}_{i}^{2} = {[(\boldsymbol{\varphi}_{j})^{\boldsymbol{T}}[\boldsymbol{K}](\boldsymbol{\varphi}_{j})} \Big/ {[(\boldsymbol{\varphi}_{i})^{\boldsymbol{T}}[\boldsymbol{M}](\boldsymbol{\varphi}_{i})} \qquad \textbf{(5. 9)}$$

The orthogonality property of normal modes ensures that each normal mode is distinct from all others. Physically, orthogonality of modest means that each mode shape is unique and one mode shape cannot be obtained through a linear combination of any other mode shapes. A natural mode of the structure can be represented by using its generalized mass and generalized stiffness. For each possible component of rigid-body motion or mechanism, there exists one natural frequency that is equal to zero. The zero-frequency modes are called rigid-body modes. Rigid-body motion of all or part of a structure represents the motion of the structure in a stress-free condition. Stress-free, rigid-body modes are useful in conducting dynamic analyses of unconstrained structures, such as aircraft and satellites. Also, rigid-body modes can be indicative of modelling errors or an inadequate constraint set. An important characteristic of normal modes is that the scaling or magnitude of the eigenvectors is arbitrary.

Mode shapes are fundamental characteristic shapes of the structure and are therefore relative quantities. In the solution of the equation of motion, the form of the solution is represented as a shape with a time-varying amplitude. Therefore, the basic mode shape of the structure does not change while it is vibrating; only its amplitude changes.

POINT normalization of eigenvectors allows you to choose a specific displacement component at which the modal displacement is set to 1 or -1. This method is not recommended because for complex structures the chosen component in the non-normalized eigenvector may have a very small value of displacement (especially in higher modes). This small value can cause larger numbers to be normalized by a small number, resulting in possible numerical round off errors in mode shapes.

Mode of vibration also helps in identify failure zones by indicating the high stressed elements. Zones of modal show high stressed have probably highly stressed of material when hopper is dynamically load condition [19].

The modal analysis of DCPD hopper is constrained system. In this situation, there will be non-zero frequency modes. If any zero-frequency are found, it is an indication that some part of the hopper model is free to move in a rigid body manner. This type of motion is generally referred as a mechanism and this problem is solved by modal analysis. A modal analysis is often used as a correcting tool for static analysis problems are failed. The source of zero frequency mode is present in this model. Model have constrained points and static analysis is done by using Finite element method.

The hopper tipper application on vehicle where it should sustain a lot of vibration from road bumps.

On-road application is subjected to road loading vibrations. Computer added engineering is effective tool to analysis of road vibration as compare to physical prototype testing in actual road conditions. Modal analysis is critical part of design process for analysis variation in different design with in a day. A number of design iteration is done to develop a perfect design to provide physical warranty of physical testing of hopper on vehicle.

Process of Modal Analysis in MSC Nastran

1¶ Open the 3D model and Start the Nastran in CAD Environment.

2¶ Defining of Physical Properties in idealization ribbon.

3¶ Change in Analysis type.

4¶ Constrain the hinge points.

5¶ Meshing of model and Run for Analysis.

6¶ Frequencies Review at different modes.

7¶ Review of Mode shapes at all frequency.

Hopper Model mode shapes defined as the relative deflections over the body structure, this is identified by the mode shape vector. The modes upto100 Hz of the body's structure, acquired using MSC Nastran, can examine virtually. First four modes of vibration are preferred for analysis of the hopper. The first mode is twisting about the longitudinal direction, which is named as torsion mode. The second mode type is bending about the vertical direction, a named twist mode. For hopper body, this mode exhibited a shearing motion at the top end, it often called a parallelogram wagon model in the vehicle industry. The third mode type is bending about the transversal direction, is called as bending mode. The bending mode showed a pushing behaviour. Floor is oscillating out of phase.

A hopper body (i.e. multidimensional body complicated than simple spring mass system) can vibrate in many different ways. Vibration of the hopper is not 'simple harmonic motion or oscillation'. These different approaches or mode of vibration will each have their own frequency, that frequency determined by moving mass in that mode, and the restoring force which tries to return that specific distortion of the body back to its equilibrium position.

It can be a little difficult to determine the shape of these modes. For example, one cannot simply strike the object or displace it from equilibrium, since not only the one mode liable to be excited in this way. Many modes will tend to excite, and all to vibrate together. The shape of the vibration will thus be very complicated and will change from one instant to the next. However, one can use resonance to discover both the frequency and shape of the mode. If the mode has a relatively high Q and if the frequencies of the modes are different from each other, then we know that if we vibration the body very near the resonant frequency of one of the modes, that mode will respond a lot. The other modes, with different resonant frequencies will not respond very much. Thus, the resonant motion of the body at the resonant frequency of one of the modes will be dominated by that single mode.

Experiment done with strings by mounted at two fixed point in tension, we analysed that the string in under a variety of modes of vibration by excitation of frequencies. In small frequency string is oscillates up and down and major movement at the centre of the string. With varying in excitation frequency two or more major movement at the different location of the string are found i.e. define the mode shape of the string.

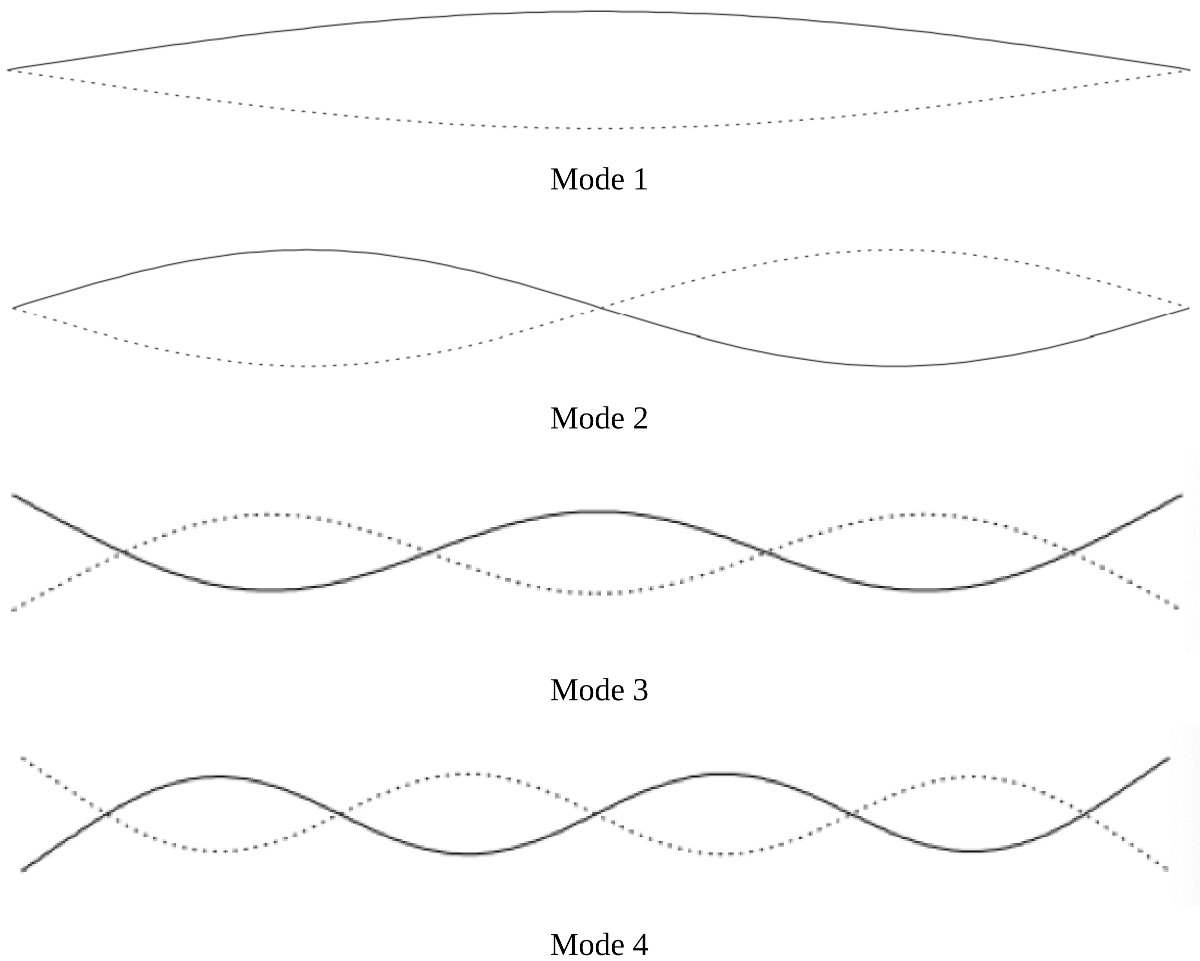

Figure 5.4: Modes of string at different frequency *(Rao, 2011)***.**

The figure shows the shape of the mode at its point of maximum vibration in one side and the dotted line is its maximum vibration on the other side.

If we increase the frequency of the oscillation become double that first modes frequency we get in the string again vibrating up and down, but with a very altered shape. At this frequency, two half of the string vibrate in opposition to each other. As one half vibrates up, the other moves down, and vice versa.

As we keep on increasing the oscillation frequency we get each whole frequency number multiple of the mode 1 frequency to next mode. At each step increase, the mode gets an extra "hump" and also an additional place where the string does not move at all. Those places where the string does not move are called the nodes of the mode. Nodes are where the quantity (in this case the displacement) of a specific mode does not change as the mode vibrates.

5.5 Global Stiffness

The global stiffness analysis is necessary for complex spring mass system; a design of the hopper body is impractical with simple spring mass system. An efficient way to design a vehicle body in different loading conditions often calculated at each stage of development as it is interconnected with vehicle attribute (chassis frame, suspension). Along these lines, it is important to assess whether this as of now utilized measure is rational for the overall vibration execution of the hopper [20]. The stiffness was calculated according to specified procedure of the TATA vehicles. The implementation of global stiffness and torsional & bending stiffness for analysing hopper body performance. In short, the hopper is constrained at fixed and resting areas in an approach to ensure a system is statically determined and a static load is applied to generate global deformations. The deflections are recorded every finite points in hopper expected to represent the global deformation of the hopper. The stiffness is calculated as

$$K = \frac{F}{\delta}$$

where,

K = Global stiffness

F = Load applied

δ = Deflection (Static deflections are calculated by using MSC Nastran)

5.5.1 Torsional Stiffness

The torsional stiffness of the hopper is measured by fixing the rear left hinge attachment in the x- ,y- and z-direction and the rear right hinge attachment in the z-direction. Also, the long-member resting part of the hopper body was fixed in order to prevent the system from becoming a moving part. Two parallel forces in the opposite direction is applied at the front left and right central axis of hopper to provide a torsion at the front zone of the body. The deflection is analysed at every finite mesh point below the centre axis of the hopper, along the vertical axis, but at the same longitudinal position at the load is applied. The deflection analysing zone was selected to minimize the influence of the local stiffness of the ribs [21].

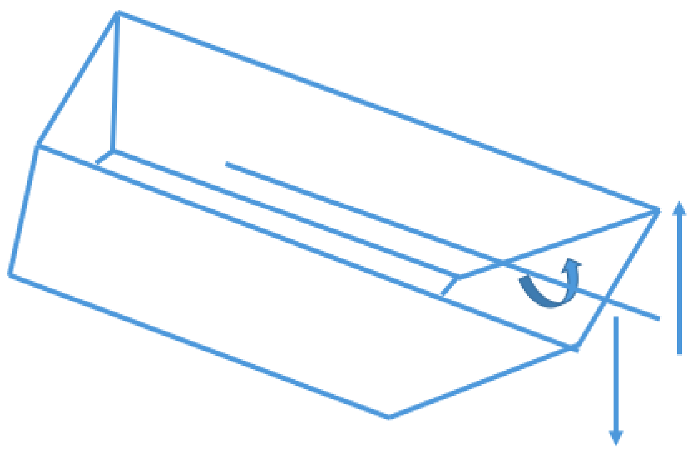

Figure 5.5: Torsional loading case of hopper.

Stiffness K is calculated as

$$K = \frac{M}{\varphi} \tag{5. 10}$$

Where,

M = Moment on hopper body

φ = Angle of deflection

These are calculated as

$$M = FL_{Load} \tag{5. 11}$$

$$\varphi = (-D_{ZLHS} + \ -D_{ZRHS})L_{length} \tag{5. 12}$$

Where,

F = Load applied

$D_{Z,LHS}$ and $D_{Z,RHS}$ are the vertical displacements on the left hand side and right hand side, respectively.

L_{Length} is the transversal distance between the two evaluation elements?

5.5.2 Bending Stiffness

The bending stiffness of hopper is measured by fixing the rear left hinge attachment in the x-, y- and z-direction, the rear right hinge attachment point in the z direction, the long-member resting part of hopper the y- and z-direction and the front right hinge attachment point in the z-direction. Two parallel forces in the same direction are applied to provide bending at the centre axis of the hopper body, i.e. one load is applied to the left front side of the body and one to the right front side of the body.

The stiffness K is then calculated as

$$K = \frac{2F}{D_{z,\,mean}} \tag{5. 13}$$

where,

F = Load applied

D_z = Mean vertical deflection of the axis assessment length along the tipping flow.

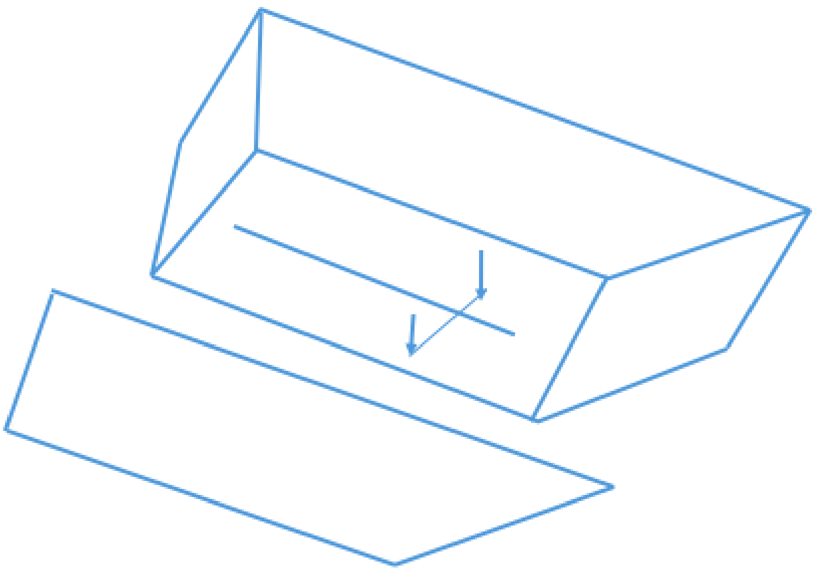

Figure 5.6: Bending force case of hopper.

5.6 Stress Analysis of hopper Tipper

DCPD hopper tipper is subjected to uniform distributed load of 1500 Kg. We do FEA of hopper floor for analysis of stress distribution. Four types of models analysed in MSC Nastran, with ribs, without ribs, supporting structure. Hopper is used as tipping so we perform stress analysis in case of different tipping angle. At tipping condition load is transfer to rear end of hopper because of gravity force acting on that. Rear part of tipper is tapered there will be stress concentration in this zone.

Stress equation of Uniform distributed loaded hinged hopper.

$$\boldsymbol{\sigma_{max}} = \frac{\mathbf{F*L}}{\mathbf{2*Z}} \quad (5.\ 14)$$

σ_{max} = Maximum stress (MPa)

F = Loading force (N)

L = Loading Span (mm)

Z = Section modulus of hopper (mm^3)

5.7 Deflection Analysis of Hopper Tipper

When the hopper is loaded with 1.5-ton uniform distribution over the floor. Deflection in hopper body main consideration for analyzing to check it should be within the elastic limit of material otherwise permanent deformation in a body. Permanent deformation is not acceptable in vehicle design and its consider as failure in hopper body.

Deflection equation of Uniform distributed loaded hopper.

$$\boldsymbol{\delta}\mathbf{max} = \frac{\mathbf{W*}\boldsymbol{l}^{\mathbf{4}}}{\mathbf{8*E*I}} \quad \mathbf{(5.\ 15)}$$

$$\boldsymbol{\delta} = \frac{\boldsymbol{W} * \boldsymbol{X}^{\mathbf{2}}(\mathbf{X}^{\mathbf{2}} + \mathbf{6l^2X} - \mathbf{4lX})}{\mathbf{24} * \boldsymbol{E} * \boldsymbol{I}} \quad \mathbf{(5.\ 16)}$$

W = Uniform distributed load (N/mm)

δ = Deflection (mm)

E = Young modulus (MPa)

I = Moment of inertia (mm^4)

L = loading span (mm)

X = length from fixed point (mm)

Chapter 6: RESULTS AND DISCUSSIONS

To test the feasibility of the manufactured DCPD hopper, the hopper model is simulated in Matlab and finite element analysis in Nastran software. Free-Free vibration with varying load and vibration due to the impact of mass is simulated in the Matlab. Modal and Stress analysis under loaded hopper is finite element analysed by using Nastran. Five different designs of hopper four of them are made of DCPD and one Stainless steel is analysed and compared to design a perfect hopper. The hopper was subjected to 1500Kg Uniform, distributed load and mounted on hinge points at the rear end.

6.1 Matlab Results

Figure shows dynamic response of Simple Single degree of freedom vibration model in matlab Simulink to investigate the damping behavior of the hopper. The amplitude of the vibration and time is noticeable actual damping coefficient and stiffness. The hopper mass, damping coefficient and stiffness are calculated 39Kg, 0.486N/(m/s) and 24.54N/m respectively. A force of 500N is applied on SDOF model sinusoidal response of vibration. The dynamic oscillation response of hopper system decay over time. Polymers are damped due to viscous damping, viscoelastic damping, friction damping and plastic deformation [20].

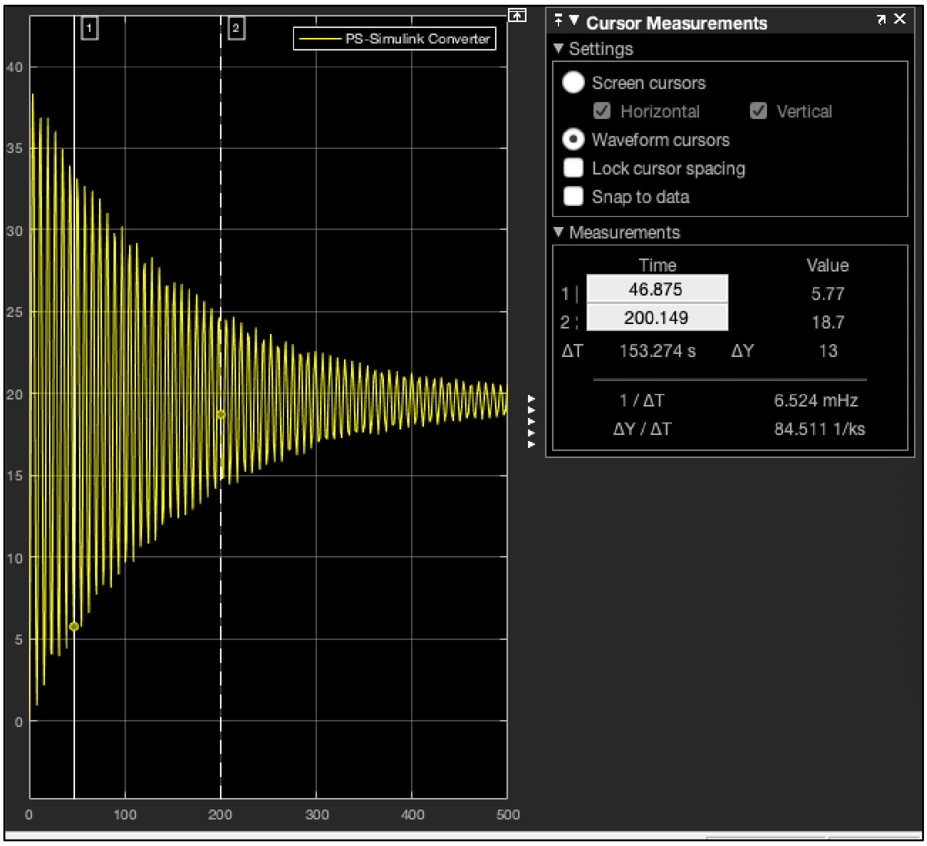

Figure 6.1: Under damped oscillation of Single degree of freedom model.

An analysis in matlab done to natural frequency at varying loading mass in hopper. By increasing mass frequency of vibration decreases sharply up to 250 Kg after that attenuation of vibration become parabolic and at the end saturation stage. Its means more mass in a hopper inclines to reduce vibration.

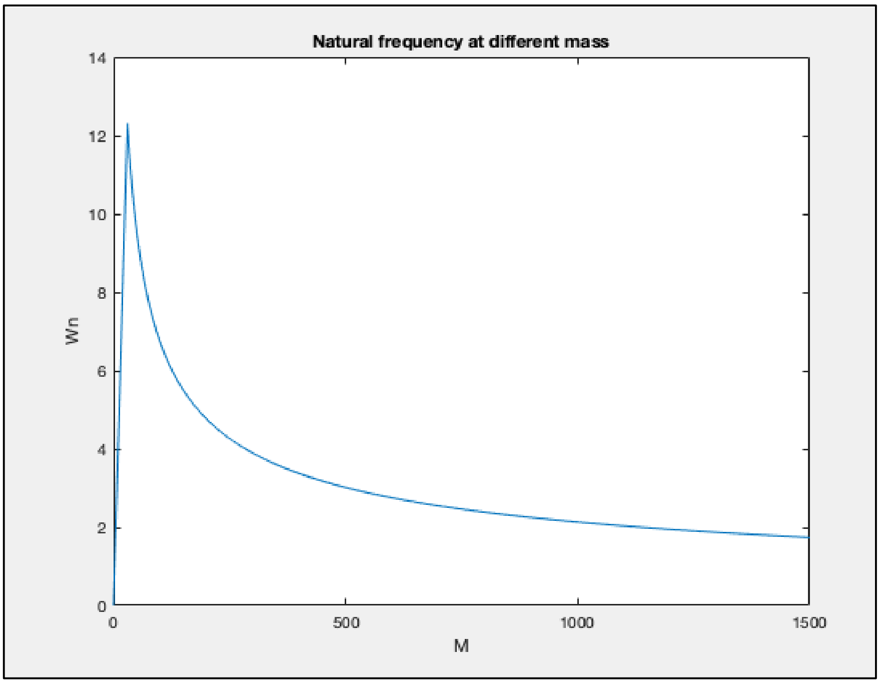

Figure 6.2: Natural frequency of vibration at different loading condition.

Figure 6.3: Graph showing time period of vibration shown in graph at different mass of loading. An analysis done to detect the Time taken in sec to come stationary condition.

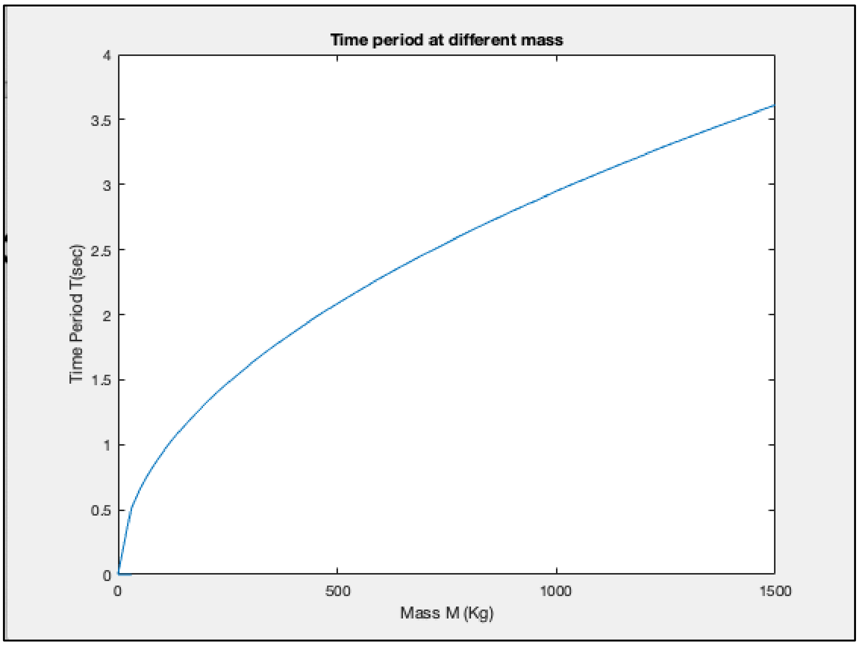

Figure 6.3: Time period of vibration at different loading condition.

To analyses of performance and behavior of vibrating system for different damping ratio. Damping constant signify how damping of vibration done in model to absorb vibration make model stable quickly. With increase in damping ratio of material damping constant is increased.

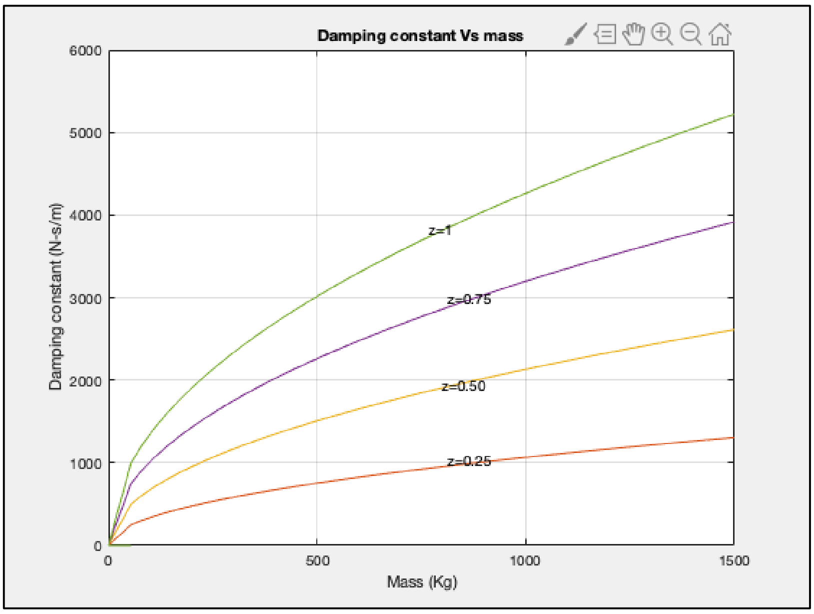

Figure 6.4: Damping constant of hopper at different damping ratio.

A mass of 0 to 100Kg, moving with velocity, strike the mass M of a damped single-degree- of-freedom. Response of impact weight on hopper it gets deflected with how much displacement measure to check inside the elastic limit of material to resist from fracture or permanent deformation. Figure shows a 30Kg mass hit the hopper will displace it by 1.582mm.

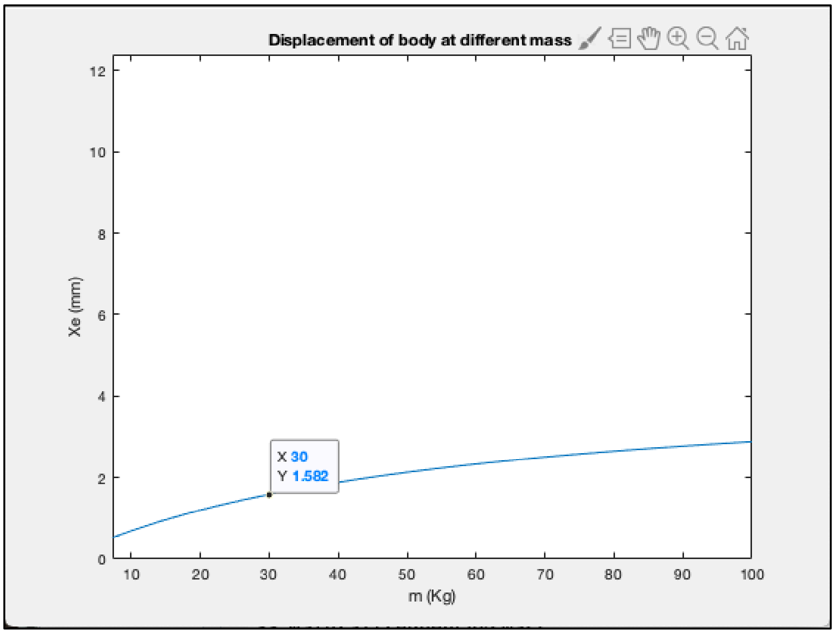

Figure 6.5: Displacement of hopper when hit by different mass at 1m.

6.2 Modal Analysis Results

The following results were obtained when hopper finite element model analyzed with finite element Nastran software.

Figure 6.6 shows the comparison of the frequency modes of the different design hoppers. Mode defines the vibrating pattern of the model at different frequency of vibration. Higher frequency means model sustains more vibration to overcome next vibrating mode. DCPD with stiffener and support is more close to Steel hopper compare to other three models. Mode 4 frequencies of vibration observed very less than Steel means mode 3 to mode 4 transfers is very quickly just increment of 1.9Hz. Without stiffener DCPD hopper is very less mode frequency which is not appropriate for hopper application or vehicle may chances of failure higher.

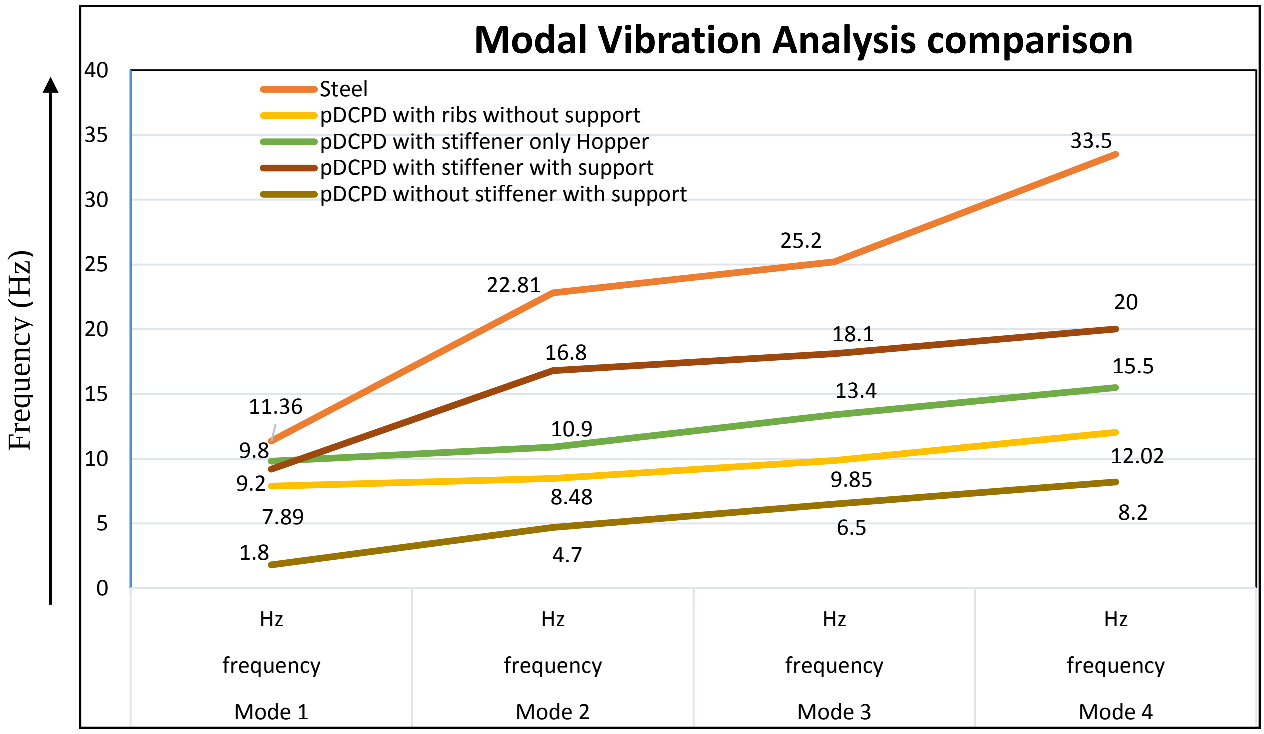

Figure 6.6: Modal vibration Analysis comparison of different models.

The comparison of modal displacement of the hoppers at different modes. The tendency for high frequency leading to more displacement observed. More displacement means chances of failure are higher due to fatigue in the material. Figure 6.7 shows steel and DCPD with stiffener with support is having very close displacement at mode 4. DCPD with ribs & without support shows inconsistent results of displacement because at the area of ribs have low displacement and more at the bottom.

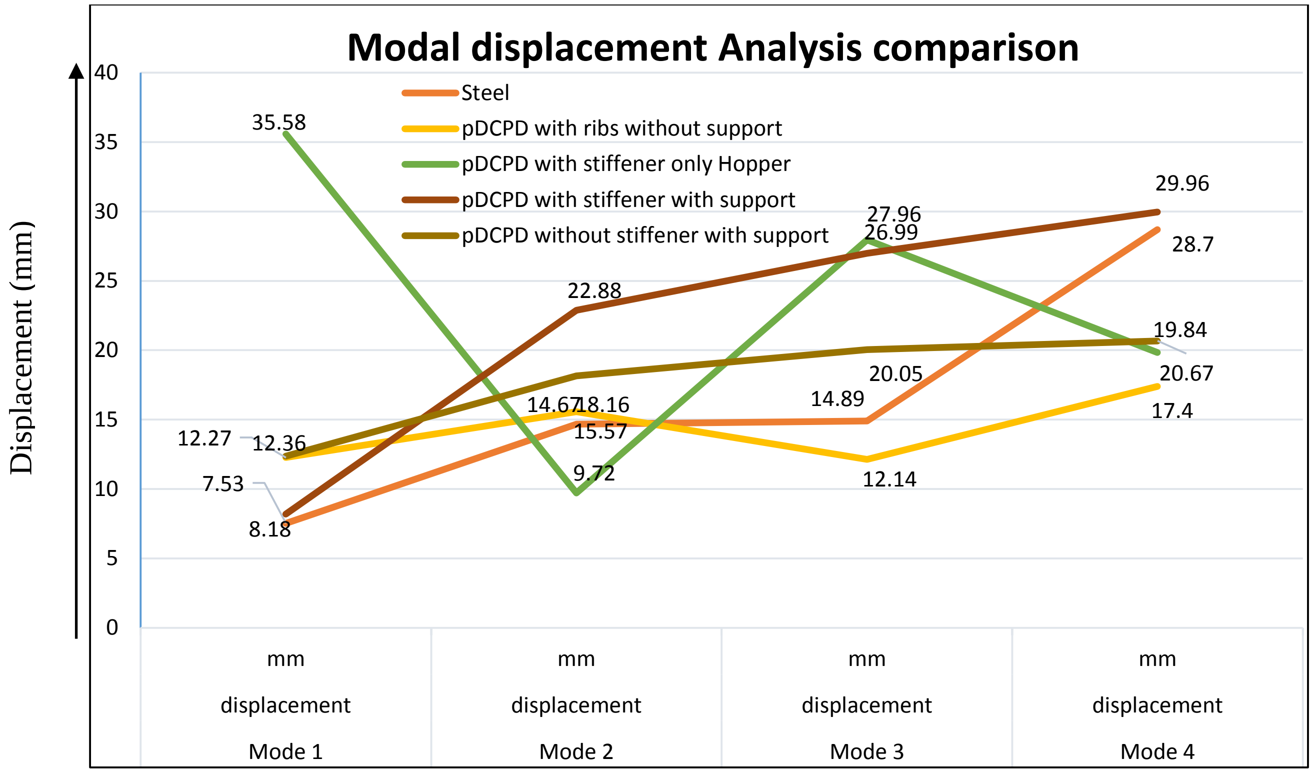

Figure 6.7: Modal displacement Analysis comparison of different models.

6.3 Load Analysis Results

Figure 6.8 shows the hopper is subjected to UDL (uniform distributed load) on cantilever beam (in tipping condition) as Stresses in Front, rear and center analysis for different designed models compared. Data of Steel hopper extrapolated for comparing with polymer designs to make them apple to apple comparison. In central region more stress because of corner shape force is concentrated high in this region. Hopper with ribs and support shows stress within the tensile strength of material. Without stiffener hopper is also within tensile limit but displacement and vibration in free-free run is higher.

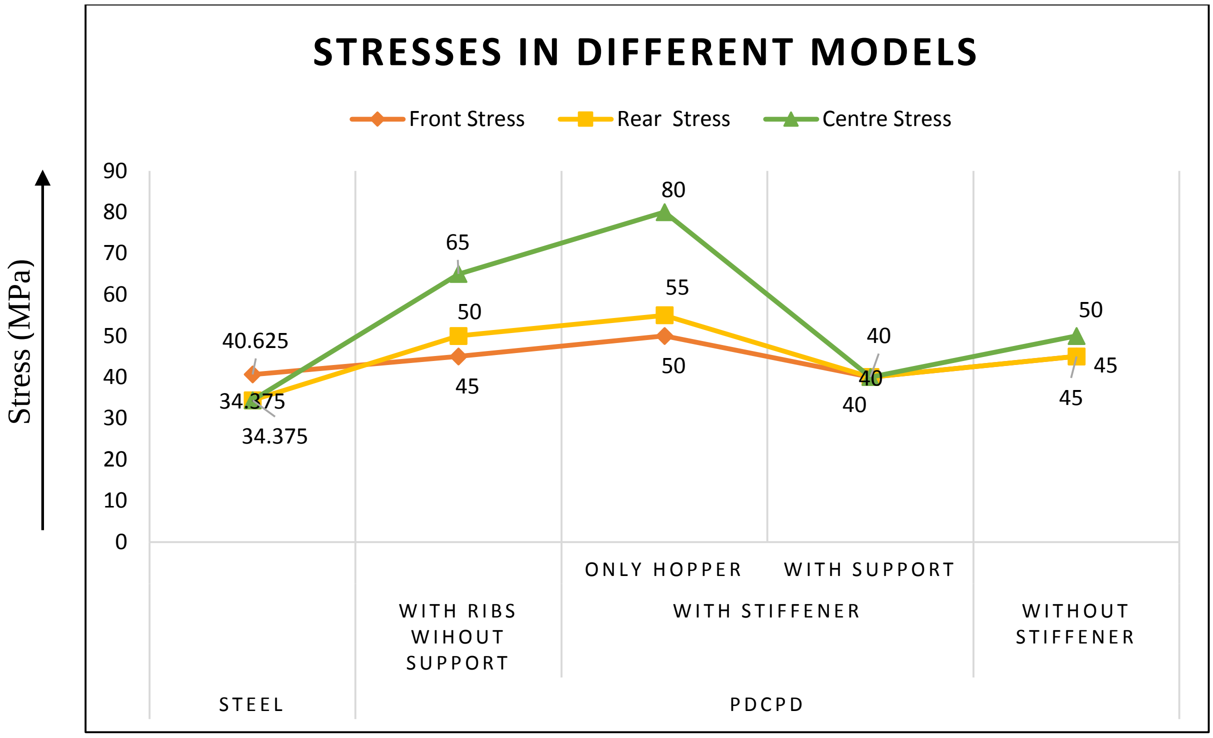

Figure 6.8: Stress comparison of different hopper models.

Figure 6.9 shows the deflection of hopper from hinge point to end, hopper is span uniform distributed loaded. Deflection in hopper is almost linearly vary from fixed point to end of the hopper. Maximum deflection of 0.128mm is calculated which is within the limit of elongation of DCPD material.

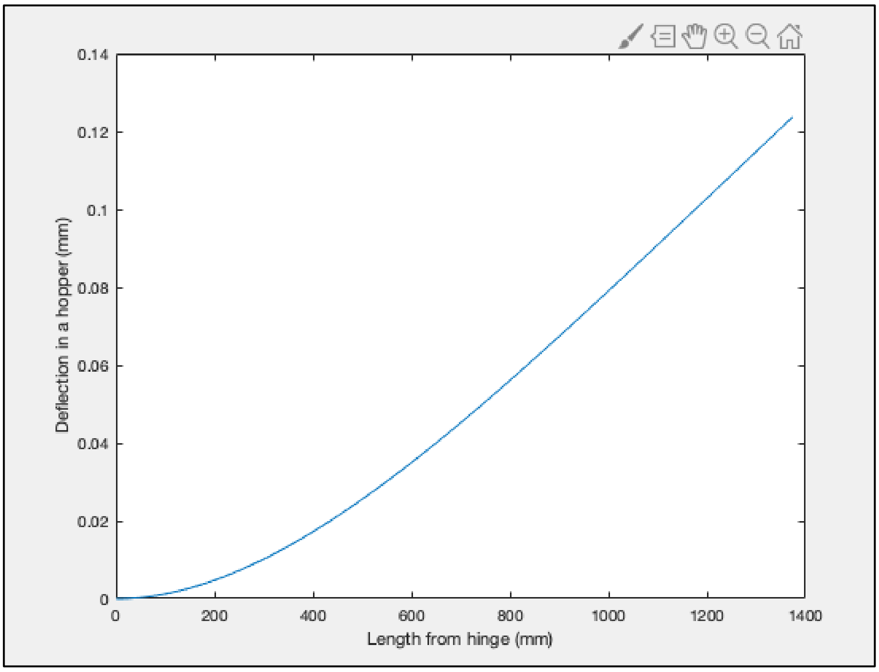

Figure 6.9: Deflection in hopper from hinge to end point at UDL.

Figure 6.10: shows the weight and thickness of DCPD, Aluminum and Steel material hopper. Weight saving of 12.1Kg (23.67%) achieved at lightest metal aluminum compare to using DCPD, without thrashing of the strength. A 35.3Kg (47.51%)weight saving compare to steel.

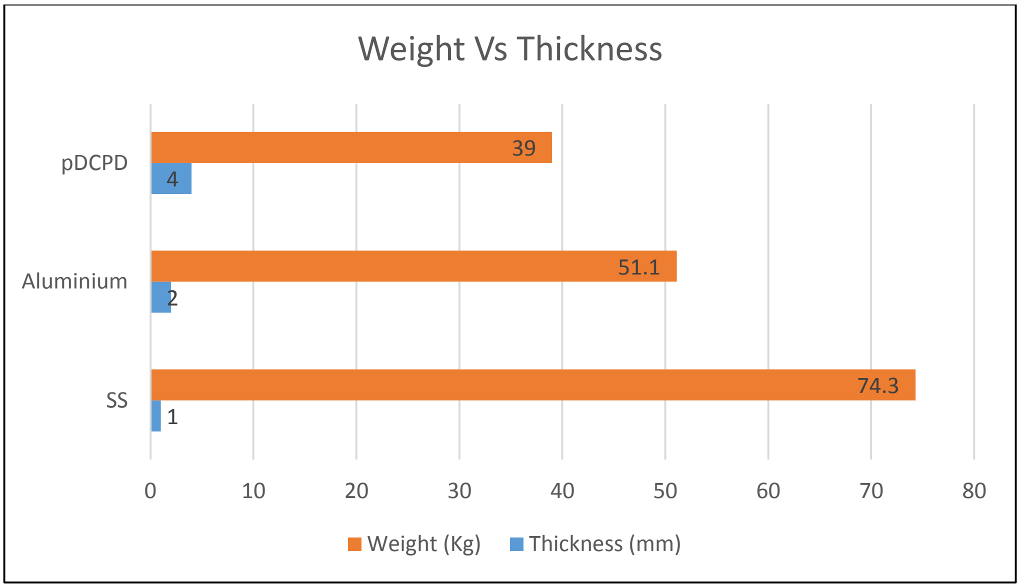

Figure 6.10: Hopper Weight comparison of Polymer, Aluminum and Steel.

Chapter 7: CONCLUSION AND RECOMMENDATIONS

7.1 Conclusion

From the above results we concluded that:
A new type of lightweight, high strength material could be used to provide a feasible design solution of a hopper tipper. This can fulfil market desire for advanced lightweight, cost efficient manufacturing process, good strength of vibrations and stresses. The wide range of chemicals resistant of DCPD makes it suitable for rough environmental conditions. Hopper made from DCPD can be handle different range of chemicals except Nitric acid and hydrogen peroxides. As a result, this research work was designed to examine an innovative solution for small commercial vehicle - a hopper tipper made from a low density material that possesses excellent chemical and mechanical properties.

At the initial development stages it could be concluded that a hopper with ribs and supporting structure is adequate to ensure the structural strength required to store 1500Kg of payload in the hopper. The maximum stresses in hopper were analysed to be upto 40 MPa at rib design with supporting structure model which is lower than the tensile strength of DCPD so hopper will sustain desire payload without failure. Shore D hardness test of DCPD showed excellent results in terms of wear resistant and scratching property which is higher than nylon roller skating wheels.

In terms of physical attributes, it is concluded that, in the final hopper, a minimum weight of 39Kg DCPD with 4mm thickness is optimum to carry the desired pay load without any failure. Same hopper of steel (1mm) and aluminum (2mm) were of 74.3Kg and 51.1Kg respectively. All three models showed equivalent stiffness however, a massive weight saving was recorded in DCPD model which accounts to 47.51% and 23.67% compared to steel and aluminum respectively without loss of stiffness of the hopper.

For prototype building, it is difficult to mould the entire hopper in a single piece using the reaction injection moulding to avoid moulding defects in a single big part. Therefore, hopper is manufactured in multi parts - LH side, RH side and centre portions then assembled by metal fasteners and adhesive. To prevent vibrations and building tearing strength of DCPD due to contact between hopper and fasteners, an adhesive between assemble components is used.

Thus, it can be concluded that DCPD RIM-based hopper could contribute towards producing a new and exciting automobile design with sufficient structural integrity, lower capital investment and adequate strength of the structure.

7.2 Recommendation and Future Works

The following recommendation and future work are identified:

- Reinforcement of glass and carbon fibre in DCPD may provide a higher strength composite material with attractive properties.
- Metal wire reinforcement technique development and validation could be explored to obtain higher strength.
- DCPD is a thermoset polymer which is yet to develop recycling or reusable options to overcome environmental concerns.
- Structural reliability of the assembly remains uncertain. Additional simulations or real tests shall be made in order to understand the adhesive acting on DCPD under different weather and fatigue conditions.
- Additional research needs to be done on the DCPD polymerization with the aim of reducing its odour, which is, apparently, a limiting factor on its massive adoption.

REFERENCES

[1] M.W. Verbrugge , T.M. Lee , P.E. Krajewski , A.K. Sachdev , C. Bjelkengren , R. Roth , R. Kirchain , Mater. Sci. Forum (2009), 618 – 619 , 411.

[2] Michael Ashby, Hugh Shercliff and David, "Materials Engineering, Science, Processing and design". University of Cambridge, UK, (2007).

[3] Płaczek M., "Comparison of vibration damping of standard and DCPD housing of the electric power steering system, IOP Conf. Series: Materials Science and Engineering", (2017), 227 012095.

[4] Margarita K. Zamanova *, "friction and Wear Behavior Of Dicyclopentadiene Under Dry Sliding And Boundary Lubrication", Pet Coal; (2016), 58(5): 556-560.

[5] James Gilford III; Marwa M. Hassan, M.ASCE; Tyson Rupnow, M.ASCE; Michele Barbato, M.ASCE; Ayman Okeil, M.ASCE; and Somayeh Asadi, "Dicyclopentadiene and Sodium Silicate Microencapsulation for Self-Healing of Concrete", J. Mater. Civ. Eng. (2014), 26:886-896.

[6] Bingli Pana b*, Jing Zhao a , Yuqing Zhang a , Yongzhen Zhangb, "Dry Sliding Behaviors of Dicyclopentadiene under Elevated Sliding Velocity", (2012), 19-24.

[7] Daniel B. Knorr Jr, "Overcoming the structural versus energy dissipation trade-off in highly crosslinked polymer networks: ultrahigh strain rate response in polydicyclopentadiene", CSTE, (2015), 6077.

[8] Andre Camboa, Bernardo Ribeiro, "A Mechanical Analysis of Dicyclopentadiene with Metal Inserts Through Flexural Load", IRF, (2013), 23-27.

[9] Shi Xiaorong, "DCPD covers part structure for car", (2018) CN207029090U.

[10] Joung-Man Park, Jin-Yeong Choi, Dong-Jun Kwon, "Improved interfacial adhesion and manufacturing method ofMGF/P-DCPD composites using W, Mo, OR Ru type catalysts in air condition", 20^{th} Internation conference on composite materials, (2015).

[11] Sherman, L.M. "Poly-DCPD RIM shifts into higher gear", (2002), 0032-1257.

[12] Davidson, T.A. and K.B. Wagener, "The polymerization of dicyclopentadiene: an investigation of mechanism", Journal of Molecular Catalysis A: Chemical, (1998), 67-74.

[13] Ng, H., "Studies of reactive polymer processing for dicyclopentadiene RIM and filled epoxy systems", Case Western Reserve University, (1992), 228.

[14] Nylon RIM Expands into Niche Applications.(2004),June 2014]; Available from: http://www.ptonline.com/articles/nylon-rim-expands-into-niche-applications.

[15] Barnes, S.E., et al., "Raman spectroscopic studies of the cure of dicyclopentadiene (DCPD)". Spectrochim Acta A Mol Biomol Spectrosc, (2005).

[16] Toplosky, V.J. and R.P. Walsh, Thermal and mechanical properties of Poly-Dicyclopentadiene (DCPD) at Cryogenic Temperatures. AIP Conference Proceedings, (2006), 824(1): p. 219-224.

[17] Fysikopoulos, A., et al., "An Empirical Study of the Energy Consumption in Automotive Assembly". Procedia CIRP, (2012).

[18] DuPont Engineering Polymers, General Design Principle-Module 1.

[19] https://www.aerospacengineering.net/vibration-analysis-nastran-sol-103/amp/

[20] J. Helsen, L. Cremers, P. Mas, and P. Sas. "Global Static and Dynamic Car Body Stiffness Based on a Single Experimental Modal Analysis Test." In: Proceeding of ISMA 2010-USD 2010. Leuven, Belgium, 2010.

[21] S. Tebby, E. Esmailzadeh, and A Barari. "Methods to Determine Torsion Stiffness in an Automotive Chassi." In: Computer-Aided Design & Applications PACE (1) (2011), pp. 67–75.

thesis_report

ORIGINALITY REPORT

12%	8%	4%	8%
SIMILARITY INDEX	INTERNET SOURCES	PUBLICATIONS	STUDENT PAPERS

PRIMARY SOURCES

1	Submitted to Thapar University, Patiala Student Paper	2%
2	www.aerospacengineering.net Internet Source	2%
3	www.byggmek.lth.se Internet Source	1%
4	www.theory.physics.ubc.ca Internet Source	<1%
5	docplayer.net Internet Source	<1%
6	eprints.uthm.edu.my Internet Source	<1%
7	Farag, M.M.. "Quantitative methods of materials substitution: Application to automotive components", Materials and Design, 2008 Publication	<1%
8	B. Shahriyari, F. Mousazadegan, M. Latifi, H. R. Pakravan. "Modifying mechanical properties of carbon textiles reinforced epoxy composite	<1%

using multi-wall carbon nanotubes (MWCNT)", The Journal of The Textile Institute, 2017
Publication

9	Submitted to Cranfield University Student Paper	<1%
10	Submitted to University of Salford Student Paper	<1%
11	Knorr, Daniel B., Kevin A. Masser, Robert M. Elder, Timothy W. Sirk, Mark D. Hindenlang, Jian H. Yu, Adam D. Richardson, Steven E. Boyd, William A. Spurgeon, and Joseph L. Lenhart. "Overcoming the structural versus energy dissipation trade-off in highly crosslinked polymer networks: Ultrahigh strain rate response in polydicyclopentadiene", Composites Science and Technology, 2015. Publication	<1%
12	www.bksv.com Internet Source	<1%
13	Submitted to Coventry University Student Paper	<1%
14	dyuthi.cusat.ac.in Internet Source	<1%
15	Submitted to University of Sunderland Student Paper	<1%

16	Alan I. Taub, Alan A. Luo. "Advanced lightweight materials and manufacturing processes for automotive applications", MRS Bulletin, 2015 Publication	<1%
17	Demirok, Ahmet, Engin Bilge Ozgurhan, Alper Agca, Necip Kara, Ercument Bozkurt, Kadir Ilker Cankaya, and Omer Faruk Yilmaz. "Corneal Sensation After Corneal Refractive Surgery with Small Incision Lenticule Extraction :", Optometry and Vision Science, 2013. Publication	<1%
18	Submitted to The University of Manchester Student Paper	<1%
19	www.nuflowbc.com Internet Source	<1%
20	inventor.grantadesign.com Internet Source	<1%
21	Witte, F.. "Degradable biomaterials based on magnesium corrosion", Current Opinion in Solid State & Materials Science, 200810/12 Publication	<1%
22	lib.ugent.be Internet Source	<1%
23	archimer.ifremer.fr Internet Source	<1%

24	Submitted to Caledonian College of Engineering Student Paper	<1%
25	McKeen, Laurence. "High-Temperature/High-Performance Polymers", The Effect of Sterilization on Plastics and Elastomers, 2012. Publication	<1%
26	William Hill, Stella Papasavva. "Life Cycle Analysis Framework; A Comparison of HFC-134a, HFC-134a Enhanced, HFC-152a, R744, R744 Enhanced, and R290 Automotive Refrigerant Systems", SAE International, 2005 Publication	<1%
27	www.jmaterenvironsci.com Internet Source	<1%
28	Submitted to PSB Academy (ACP eSolutions) Student Paper	<1%
29	Submitted to Universiti Malaysia Pahang Student Paper	<1%
30	hik-consulting.com.pl Internet Source	<1%
31	www.dtic.mil Internet Source	<1%
32	hal-upec-upem.archives-ouvertes.fr Internet Source	<1%

33	Submitted to Universiti Teknikal Malaysia Melaka Student Paper	<1%
34	usir.salford.ac.uk Internet Source	<1%
35	Submitted to Middle East Technical University Student Paper	<1%
36	Submitted to University of Birmingham Student Paper	<1%
37	Submitted to Swansea Metropolitan University Student Paper	<1%
38	Submitted to University of Wollongong Student Paper	<1%
39	Submitted to University of Newcastle upon Tyne Student Paper	<1%
40	dr.ntu.edu.sg Internet Source	<1%
41	www.nbk1560.com Internet Source	<1%
42	Submitted to Imperial College of Science, Technology and Medicine Student Paper	<1%
43	"Dynamic Behavior of Materials, Volume 1", Springer Science and Business Media LLC,	<1%

2011

Publication

44	Submitted to University of Strathclyde Student Paper	<1%

Exclude quotes	On	Exclude matches	< 10 words
Exclude bibliography	On		